1986/1987 PROGRESS REPORT

FOR COOPERATIVE AGREEMENT NCC2-345

WITH

SAN JOSE STATE UNIVERSITY FOUNDATION
ONE WASHINGTON SQUARE
SAN JOSE, CA 95192-0139

"The Spectroscopic Chemical and Photophysical Properties of Martian Soils and Their Analogs"

MARS EXOBIOLOGY RESEARCH CONSORTIUM

Dr. Lelia M. Coyne

APPENDIX B PROGRESS

NEAR INFRARED REFLECTANCE ANALYSIS

DEVELOPMENT OF SAMPLE PREPARATION/PRESENTATION PROTOCOL

Introduction

Reflectance spectra contain information not only about the absorbance of a sample, i.e. its electronic and vibrational transitions, but also about its light scattering characteristics. The scattering is affected, not only by sample composition, but also by factors associated with sample orientation, packing density, particle size distributions and others. In addition, the efficiency of collection of the scattered light is also affected by relative placement of the source, detector and sample.

Instrument

A decision was made to purchase the Mark II 6250 Near Infrared/Visible Research composition Analyzer from Gardner Neotec. The equipment was received in part in November of 1985. Installation and initial calibration was completed in April, 1986.

Sensitivity of the spectra to minor variations in sample placement and planarity with respect to the plane of the detectors has been minimized by our choice of a single beam instrument with $0/45^{o}$ illumination/detection, rather than a double beam instrument with an integrating sphere. Even so, the net effect of the innate sensitivity of scattered light to geometrical factors standardly results in spectra which are superposed on offset, sloping and, in some cases, non-linear baselines. For these reasons it is important to develop methods for measuring the spectra which are as reliable and reproducible as possible. These methods include sample preparation techniques and means for presenting the samples to the instrument for measurement.

Sample Preparation

Three replicate samples of each material to be examined were weighed to an amount just adequate to fill a stainless steel planchette with the crude material after pressing. They were placed in the die of a pellet press and covered with the inverted stainless steel planchette. They were pressed for 30 seconds against a glass optical flat using a pressure of 1.2 kgm/cm^2 at the piston head in order to form a compact, but soft, pellet. As the density of the materials varied after the chemical treatment, some of the planchettes were overfilled by the amount used. These samples were struck off with a stainless steel blade, reweighed and the pellet re-pressed upright against the flat to smooth the surface. The filled planchette was centered on a spring-loaded platform in the lower half of a Pacific Scientific sample holder, then covered with a thin quartz cover plate that has been sealed into a screwcap. The samples, after placement in the sample holder, appeared smooth, but some surface roughness may have resulted from the striking-off precedure. The reflectance spectra were measured in the near-visible region of the near infrared from 600 to 1100nm.

Sample Presentation

In order to minimize spectral variations resulting from sample placement, several reflectance curves were measured for each sample and the results averaged. The measurements included in the average were derived from the following presentation protocol:

a) Insert planchette in sample holder. Insert holder into the drawer with a marked orientation. Measure and average 50 replicate scans.

b) Retract sample drawer to remove the sample from the light beam, reinsert without reorientation and re-measure 50 replicate scans.

c) Retract sample drawer, rotate sample holder 90^{o}, reinsert and re-measure.

d) Rotate an additional 90^{o} to 180^{o} from original orientation and re-measure.

e) Rotate to 270^{o} and remeasure.

f) Remove sample holder from drawer, sample from holder and reorient sample at random. Replace sample in holder, in drawer, reinsert and re-measure.

The spectra shown in the following figures thus represent the average of 6x50 = 300 scans of each material. A 10 point smooth using 1 nm segments has been performed on the original data, in preparation for derivatization. Features of the derivative spectra are more subject to distortion and artifact resulting from noise than are the reflectance spectra and thus the smoothed curves give more reliable regressions than do the untreated data.

In **Figure1,** smoothed spectra of three replicate samples of crude SWY-1 montmorillonite are compared with the spectrum obtained from the average of these three and with the spectrum obtained by averaging these same three spectra with three additional ones obtained after three rotations of one of the replicates of 90^{o} each. These two comparisons show the repeatability of replicates and the variability of the spectral information with sample loading.

More attention may be paid to developing practically applicable means to minimize

SWY MONTMORILLONITE–VARIABILITY OF 1/R WITH SAMPLE POSITION AND BETWEEN REPLICATE SAMPLES

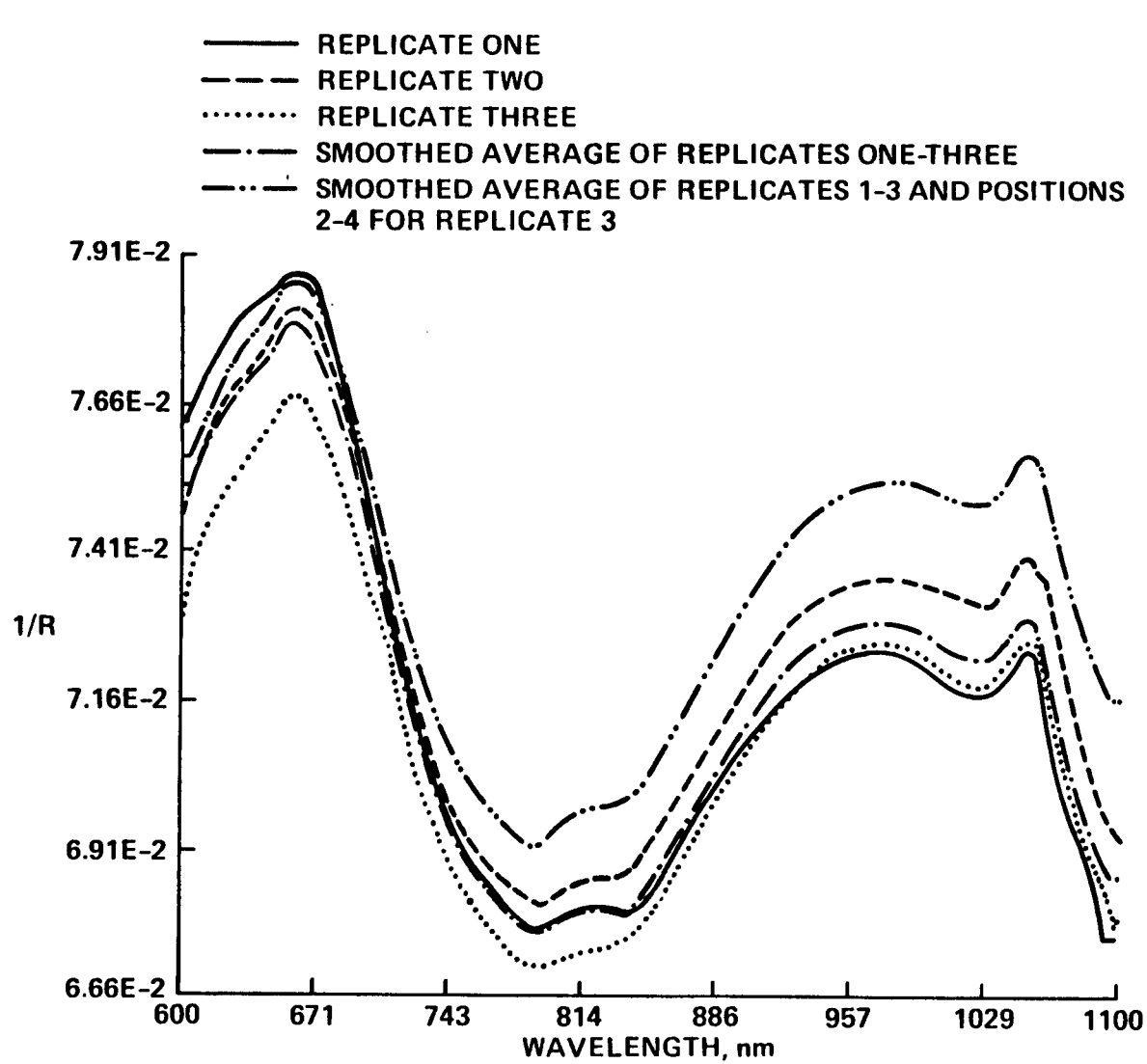

Figure 1

surface and orientational variability among large numbers of replicate and related samples of non-identical materials, just to understand the degree of sensitivity of the spectrum to these preparational variations. It should be recognized, however, that reflectance data from planetary surfaces will have to be comparable to laboratory data and deciperable without this fine degree of control over the experimental surface.

For the above reason, we have compared the above 1/R data with that obtained by taking its first and second derivatives. The resultant derivative spectra for **Figure 1** are shown in **Figures 2 and 3.** First derivative spectra were taken using 10nm segments and a gap of 10 nm between segments. Second derivative spectra were taken using 20nm segments and no gap between segments. Baseline offsets are removed by the first derivative, a constant slope in the baseline removed by the second derivative. Derivative data is clearly much more quantitatively comparable than that from the 1/R curves. The conclusion is that visual pattern recognition, i.e., attribution of the pattern-determining features, is most easily approached by examination of the 1/R data, but that first or second derivative data will likely prove more reliable for choosing a reliable analytical wavelength(s).

Optimization of Sample Dimensions

The MarSAM's are difficult to prepare in large quantities and there are several environmental parameters that must be varied in order to give a thorough profile of the spectral changes produced by varying those environmental conditions which are expected to be spectrally significant and which are uncertain for Mars. The number of samples of any given material which must be measured in order to give data at several temperatures, humidities, redox levels and energy content, in replicate, is large.

On the other hand, natural mineral samples can be inhomogeneous, and the signal to

SWY MONTMORILLONITE–VARIABILITY OF 1ST DERIVATIVE OF 1/R WITH SAMPLE POSITION AND BETWEEN REPLICATE SAMPLES

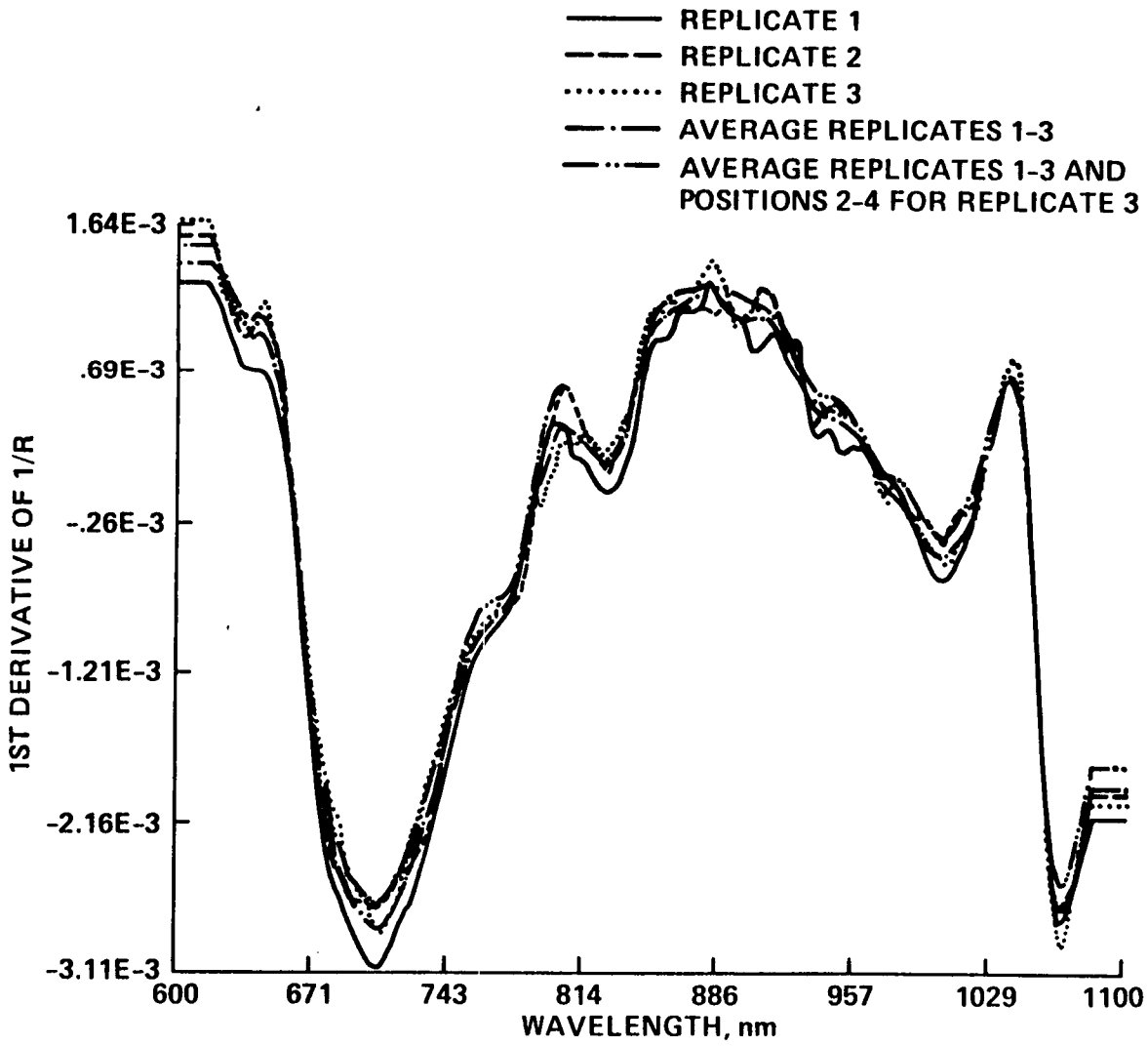

Figure 2

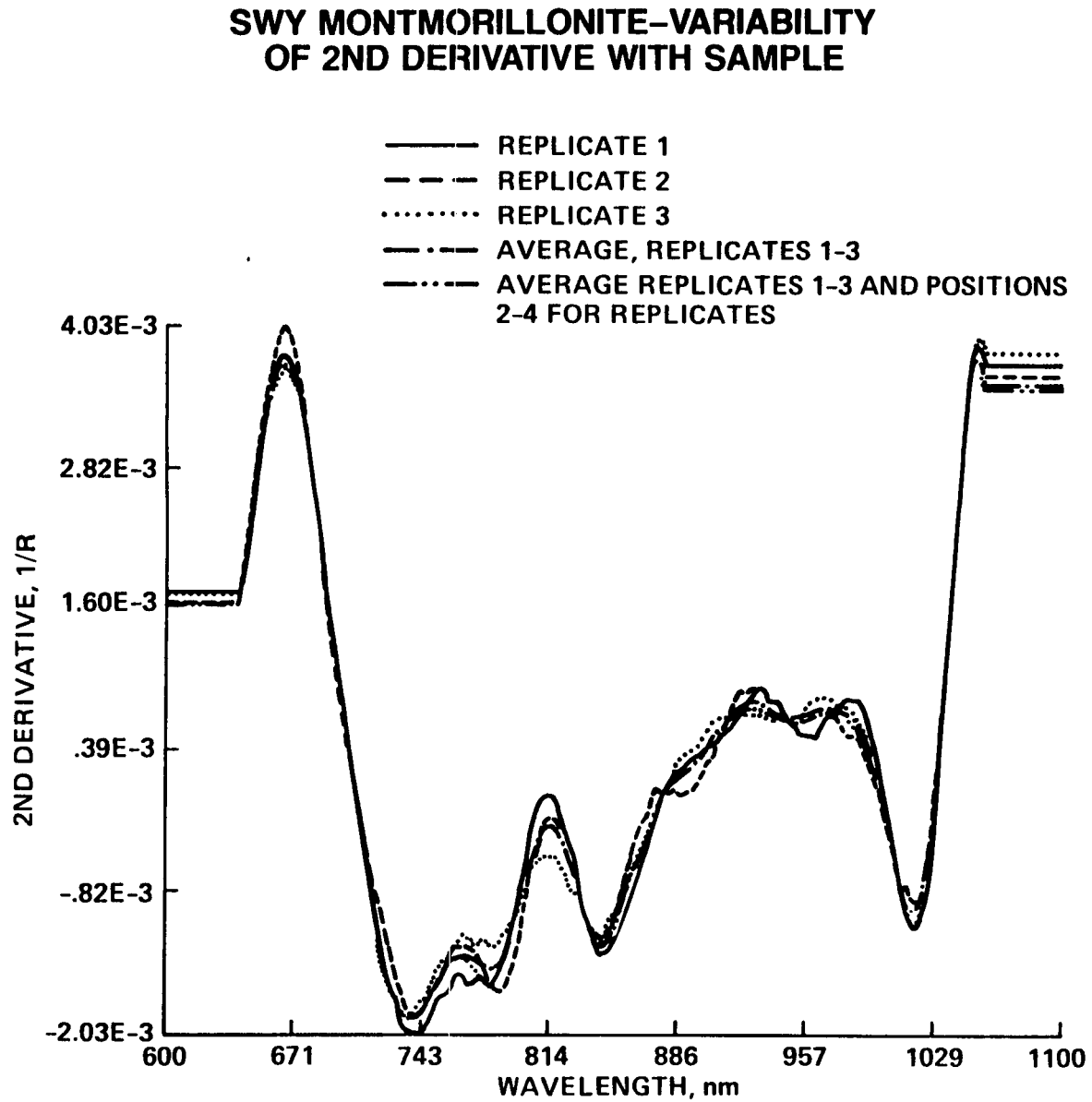
SWY MONTMORILLONITE–VARIABILITY
OF 2ND DERIVATIVE WITH SAMPLE
REPLICATE 1
REPLICATE 2
REPLICATE 3
AVERAGE, REPLICATES 1-3
AVERAGE REPLICATES 1-3 AND POSITIONS
2-4 FOR REPLICATES
4.03E-3
2.82E-3
1.60E-3
.39E-3
-.82E-3
-2.03E-3
2ND DERIVATIVE, 1/R
600
671
743
814
886
957
1029
1100
WAVELENGTH, nm

Figure 3

noise ratio in diffuse reflectance measurements is increased by collecting light reflected off a large sample area. For these reasons, the diameter of the sample, relative to the size of the impinging light beam, must be maximized.

The accurate calculation of absorbance from reflectance is based on the attainment of an infinite optical path. Rock clays are transparent to several centimeters in this region of the spectrum, though produce considerably less scattering of the light than the powders we are using. In industrial practice, where sample availability is less of a consideration than for our research preparations, the typical thickness is from 5-10 mm, - 8 mm in the press obtained from English China Clays used (with appropriate modification) for the preparation of our samples. A sample of 8 mm thickness would present problems for us in equilibration of the pellet with water and atmospheric gases, in addition to the problem of preparing a sufficient quantity of material. Therefore, the thickness of the sample must be optimized so as to to guarantee both infinite optical depth and minimal environmental equilibration time using conservative amounts of material.

Using crude SWY-1 montmorillonite as a standard and making measurements in the near-visible portion of the near-infrared spectrum, a set of sample dimensions was determined which seems optimal, for our initial environmental studies. Data were collected as a function of sample diameters ranging from 3/4" to 1 1/4" and for sample thicknesses ranging from 1-5 mm.

Sample Diameter - Spectra taken from samples in 1 1/4"and 1" planchettes were more or less equivalent, but when the sample diameter was reduced to 3/4", the noise level was increased and the peak intensity distribution was significantly altered, even though the sample is still larger than the 5/8" source beam size.

Sample Thickness - There appears to be no significant effect of sample thickness over the range of thicknesses of 1-5 mm, regardless of sample diameter. However, all the measurements were done under ambient conditions. Samples equilibrated to and measured at lower temperatures may shrink and crack, producing areas with less than the requisite infinite optical depth. Also, the crude clay studied here is more absorptive than the refined, calcium-exchanged, material that serves as the end member of our series. For these reasons, it was decided that 2 mm would provide the minimum safe thickness.

The sample dimensions determined by these measurements represent a starting protocol which provides a reasonable accomodation between the numerous conflicting priorities. However, the protocol at this point is seen as interim, because the conclusions of this study are confined to a small portion of the spectrum to be examined and require verification in other spectral regions, for more reflective clays and at other temperatures, and humidities.

Optimization of Instrument Configuration

The absorption (reflectance minima) occurring in the wavelength region shown is very weak. The sensitivity of the Neotec instrument is sufficiently high that an instrumental artifact shows up that was not observed in the spectra determined using the Perkin-Elmer multirange spectrometer. Using the midrange grating, we initially observed a signal which appears like the derivative of an absorption peak centered at about 790 nm. The Wood's anomaly (Hamilton, et al., 1978) of the grating, occurs at 770 nm. The artifactual signal we see may be entirely attributable to the Wood's anomaly, or there may be an additional contribution from the fact that the particle size of the samples being measured is comparable to the wavelength of the measuring light. This anomalous signal can be reduced to a level where our spectra are not significantly distorted by it by

diminishing the size of the impinging light beam, using an adjustable optics barrel placed between the source and the sample. There results, however, a certain cost in terms of decreased signal/noise. Further efforts to understand the determinants of this spurious signal will be made. A possible means to correct for it by subtracting a spectrum of highly reflecting particles of a standardized and matching particle size range will be developed, if need be, for use under measurement conditions where it can not be avoided.

Design of the Environmental Cell

In consultation with Peter Wood of San Jose State University and Tom Scattergood, SUNY, Stony Brook, a micro-environmental sample compartment was designed for our small clay samples.

Contact between sample and a regulated gas flow requires introduction of a gap between the sample surface and the quartz cover plate. Such a gap would produce a supervening refractive/reflective interface; change the position of the sample surface relative to the optical plane, thus affecting the focus of the illuminating beam; and, to a modest extent, affect the solid angle for collection by the detector. Before initiating fabrication, a series of tests was run to ascertain the effects of this gap on the quality of the spectral data. These tests were run at all settings of the optics barrel and for both the 3/4' and 1" planchettes. It was found that the Wood's artifact was regularly increased as a function both of gap thickness and of increasing beam size, but much more rapidly for the 3/4" than for the 1" planchette. However, using a stopped down beam, the introduction of a 1 mm gap does not appear to deteriorate the data noticeably. Studies of the effect of gap variation between 1 and 3 mm for the 1" planchette with the stopped down beam showed that, If anything, the signal to noise is improved in this configuration, but insufficient study has been done to verify the reliability of this improvement.

A diagram of the environmental cell designed by Peter Wood on the basis of these considerations and studies and fabricated at San Francisco State is shown in **Figures 4 and 5**. Temperature control will be provided by a circulating temperature bath which cools a brass mounting base in direct contact with the stainless steel planchette. Pre-cooling the stream of environmental gas is achieved by passing it through the same bath. Humidity of the gas flow will be regulated using mass flow controllers. Completion and testing of this cell is scheduled for fall of 1987.

Summary of Optimal Sample Presentation Conditions

To insure that the 1/R data is representative of sample absorbance, rather than of those reflectance differences produced by variability in surface characteristics it is preferable to run samples in replicate, in multiple orientations and after unloading and reloading. This latter precaution will be difficult to enforce when the environmental cell is in operation, but can be compensated for by use of multiple samples.

For our particular measurements, samples will be contained in a stainless steel planchette of dimensions 1" diameter by 2 mm thickness, the optics barrel opened no more than 1/4 of the way, unless provisions are taken to correct the spectra for the polarization artifact, and with a gap between sample and quartz cover plate not to exceed 2 mm. Re-verification of the validity of these operating conditions will be undertaken in other spectral regions and with the Ca-montmorillonite from both SWY and Otay parent materials, when adequate amounts of this material becomes available for study.

ENVIRONMENTAL CELL FOR DIFFUSE REFLECTOR SPECTROMETER
(DISASSEMBLED, SIDE VIEW)

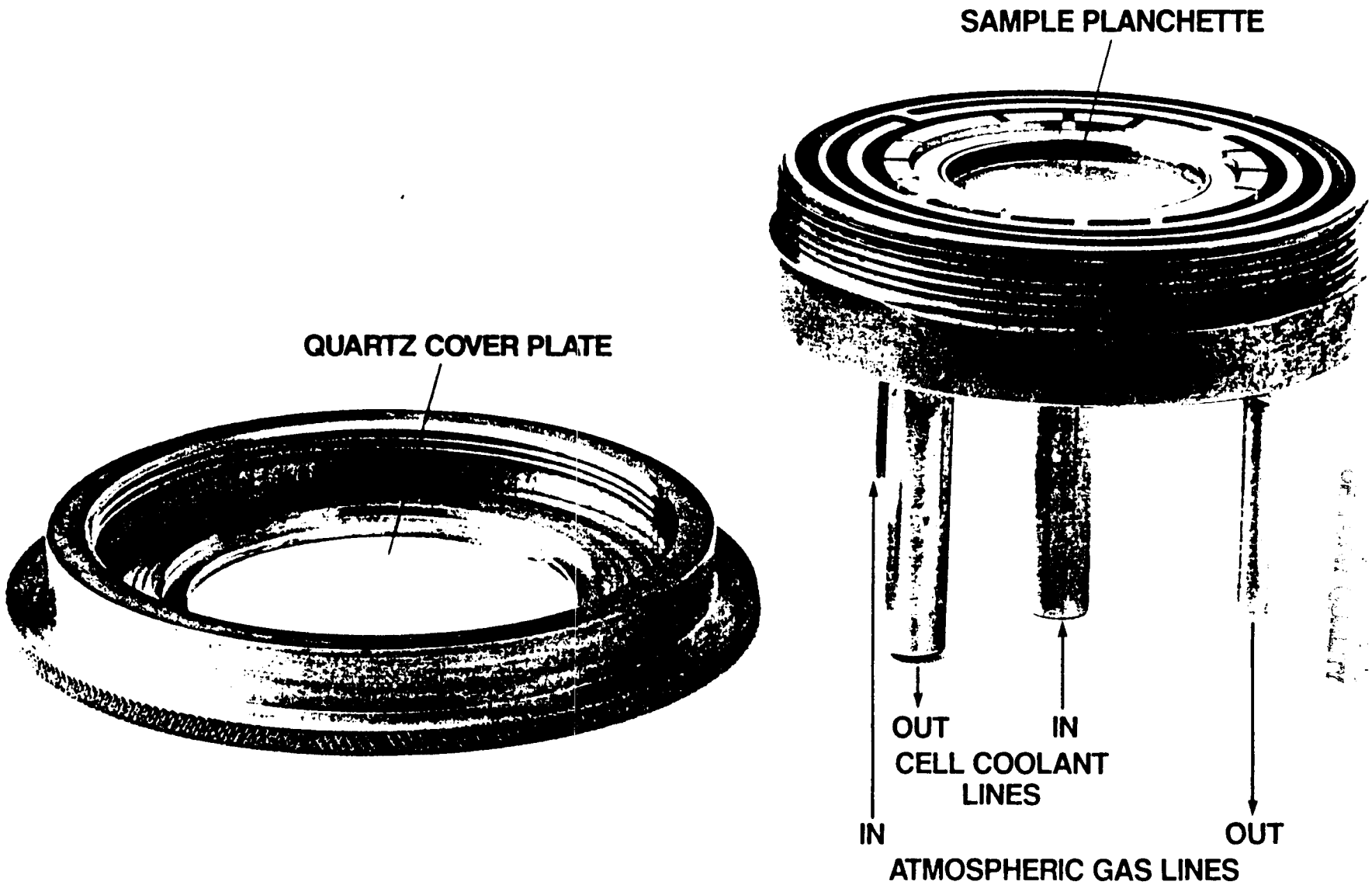

Figure 4

ENVIRONMENTAL CELL FOR DIFFUSE REFLECTANCE SPECTROMETER
(DISASSEMBLED FOR VIEW SHOWING ATMOSPHERIC GAS FLOW PATH)

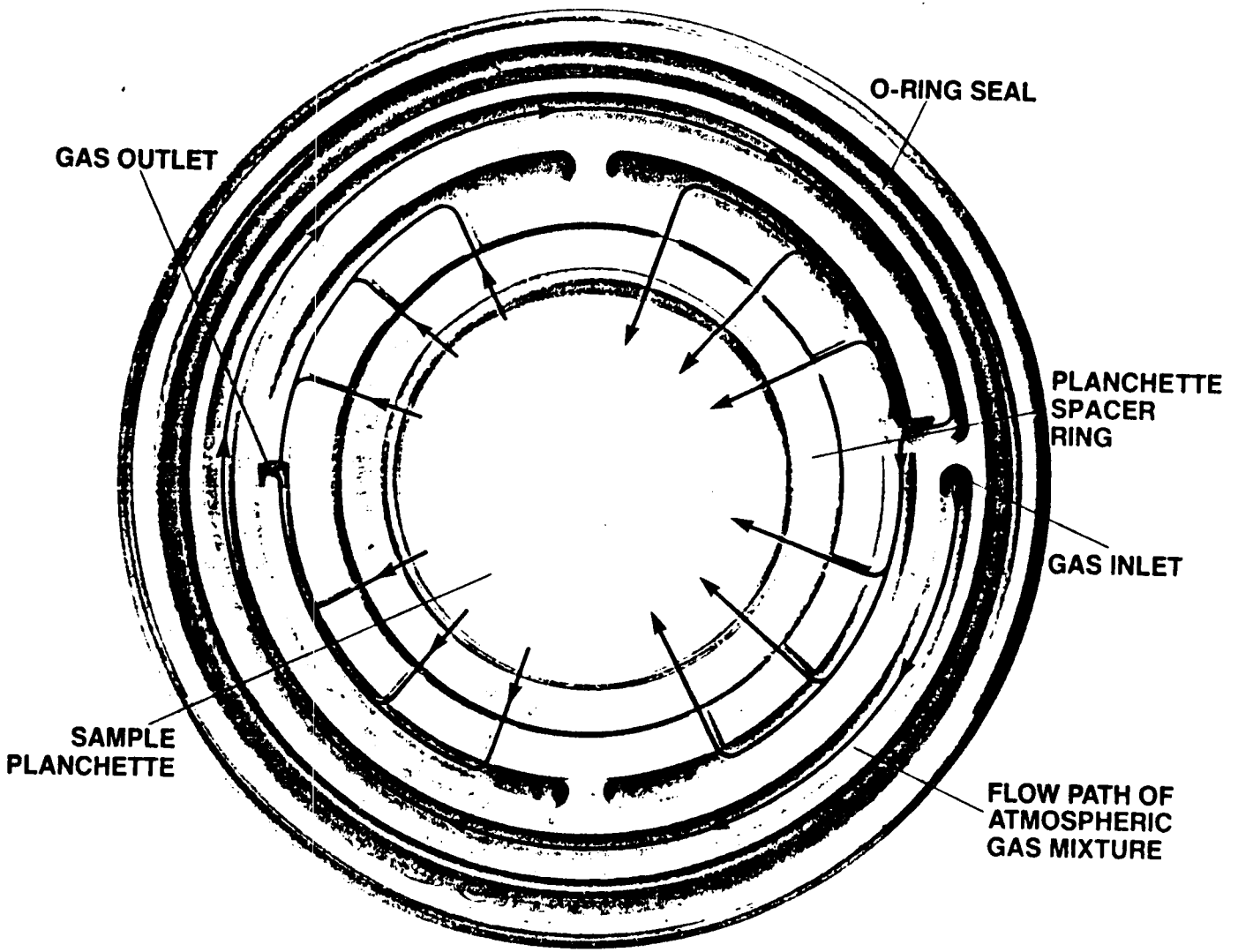

Figure 5

NEAR IR ANALYSIS (NIRA) OF 1985 MARSAMS

Method

Reflectance spectra in the near-visible portion (600-1100nm) of the near-infrared spectrum were run on the 1985 set of MarSAMs. Visual inspection of the survey spectra of these materials run on the multirange, double beam, instrument revealed two regions where there was a variability which was clearly dependent on the increased iron loading. These were in the charge transfer region extending redwards from the uv and in a barely discernable peak at about 970.

This wavelength region was selected for the initial assessments of the performance of our new instrument and the potential utility of NIRA in characterizing the reflectance signal of surface iron for several reasons. The standard grating for the Neotec instrument allows the region from 2500-680nm to be observed if scans are recorded in both first and second orders of the grating. The region from 2500 to 1100 nm is of importance, because transitions characteristic of hydroxyls, both in the clay structure and of the water of hydration of the exchangeable cations on the surface, are in this range. However, the transitions of the structural hydroxyls will be sensitive to variations in the concentration of structural iron, rather than the surface iron which is the prime variable in the MarSAM set. Past work has shown that there is no reason to expect any major differences in the extinction coefficients for OH associated with Ca as opposed to Fe and that the differences in the wavelength positions of OH for various exchangeable cations are minimal (Cariati, et al., 1983). For these reasons, it is not to be expected that the hydroxyl region will provide a particularly effective analytical wavelength for surface iron. The region from 1235 to 680 nm can be scanned using the 2^{nd} order of the near ir grating. However by 680 nm, the intensity of the C.T. transition is weak and rapidly

diminishing. For these reason it was decided to use the midrange grating instead in order to extend the range farther into the visible (1100-600).

Use of this region of the spectrum allows for simultaneous testing of the quantitative capabilities of the instrument using both of the surface iron-sensitive features revealed by the overview spectra. The c.t. band, because this transition is fully allowed, will be sensitive to total iron. The 970nm peak, barely discernable using the multirange spectrophotometer is a respectable feature on the Neotec because of the high signal to noise capabilities of this instrument. It is furthermore interesting, in that, at this sensitivity, it is clearly revealed to be a composite of two peaks, a broad one at ~970 nm and a more narrow one at ~1028, only the former of which shows a sensitivity to the iron content. That the peak is a weak composite makes it an ideal candidate for testing the quantitative analysis capabilities of the instrument under optimally unfavorable conditions of detection.

The peak at 970, most likely a forbidden d-d transition of ferric iron, may be more uniquely characteristic of the surface iron than of overall iron, or in itself the composite of peaks from structural and surface iron. It is of interest to find transitions which aid in the discrimination of structural and surface iron components, so that they can be independently assessed. In this way a new criterion by which clays may be identified, or by which iron can be associated with clays as opposed to other iron bearing minerals can be identified.

The full suite of samples examined consisted of: two replicate samples of crude SWY montmorillonite which was used as a parent material; five variably Fe/Ca-exchanged materials (0-100% nominal exchangeable iron), prepared from the SWY using the acid pre-treatment and ion-exchange refinement technique of Banin (1973); a 100%

Fe-exchanged clay, also prepared from SWY, but in 1982, in order to spot-check stability of the sample preparation technique; a sample of crude Otay montmorillonite, to be used as the parent material for a second suite of variably exchanged clays which have a lower structural iron content; and a 100% Fe-cation-exchanged derivative of the Otay sample. Analytical data on the elemental composition, most particularly the total iron content, was provided by James Orenberg, of SFSU, from the results of energy-dispersed x-ray fluorescence and inductively coupled plasma analysis of the materials. The results of the major elemental analysis are shown in **Table One**, the iron analysis in boldface. The nominal exchangeble iron is also included in the heading.

Results

Spectra for the five variably-exchanged SWY samples are shown in **Figure 6a** and for the miscellaneous remaining materials of the full set in **Figure 6b.**

Several trends are clearly apparent from visual inspection of the 1/R data for the five variably cation-exchanged materials prepared by the same method from the same parent material. Discernable absorption increases (reflectance decreases) are produced by increasing surface iron in two regions of the spectrum examined. First, the charge transfer tail is still prominent, though of rapidly diminishing intensity over the wavelength region from 600nm to longer wavelengths. It is manifested by a steep slope with an inflection point in comparison to the spectrum of the Ca-clay, which shows a maximum at 643 nm. The steepness of this slope is increased in the high iron samples. As mentioned earlier,the broad component of the peak centered around 970 nm also appears diagnostic of increasing surface iron. Furthermore it is revealed to be composed of two substituent peaks, a broad one at ~970 nm which is responsive to iron and a more narrow one at ~1028 nm, which is not.

MarSAM 85 ANALYSIS BY XRF

(% BY WEIGHT)

	9	1	2	3	4	5	6	7	8
Element	**CRUDE SWY-1**	**0% Fe 100% Ca**	**20% Fe 80% Ca**	**50% Fe 50% Ca**	**80% Fe 20% Ca**	**100% Fe 0% Ca**	**100% Fe 1982**	**0% Fe OTAY**	**100% Fe OTAY**
SiO_2	57.2	53.7	53.6	54.0	53.7	54.6	(55.7) 52.7	48.9	48.9
Al_2O_3	17.9	17.3	16.8	16.6	16.4	16.8	16.3	13.8	13.8
TiO_2	0.11	0.09	0.27	0.08	0.32	0.22	0.34	0.42	0.14
Fe_2O_3	**3.61**	**3.87**	**4.11**	**5.21**	**5.96**	**6.08**	**6.87**	**1.11**	**3.54**
MnO	0.02	<0.01	<0.01	<0.01	<0.01	<0.01	<0.01	0.03	0.02
MgO	2.66	2.15	2.03	1.90	1.94	2.03	1.92	6.88	5.71
CaO	1.62	1.41	1.73	0.94	0.47	0.14	0.17	1.07	0.15
Na_2O	1.41	0.20	0.10	0.24	0.11	0.10	0.14	0.70	0.16
K_2O	0.50	0.10	0.21	0.33	0.31	0.32	0.36	0.19	<0.10
P_2O_5	0.04	<0.01	<0.01	<0.01	<0.01	<0.01	<0.01	<0.01	<0.01
LOI	13.3	19.9	19.9	18.7	18.2	17.8	17.4	23.8	28.4
TOTAL	98.37	98.65	98.77	98.03	97.43	98.11	(99.22) 96.22	96.91	100.93

Table 1

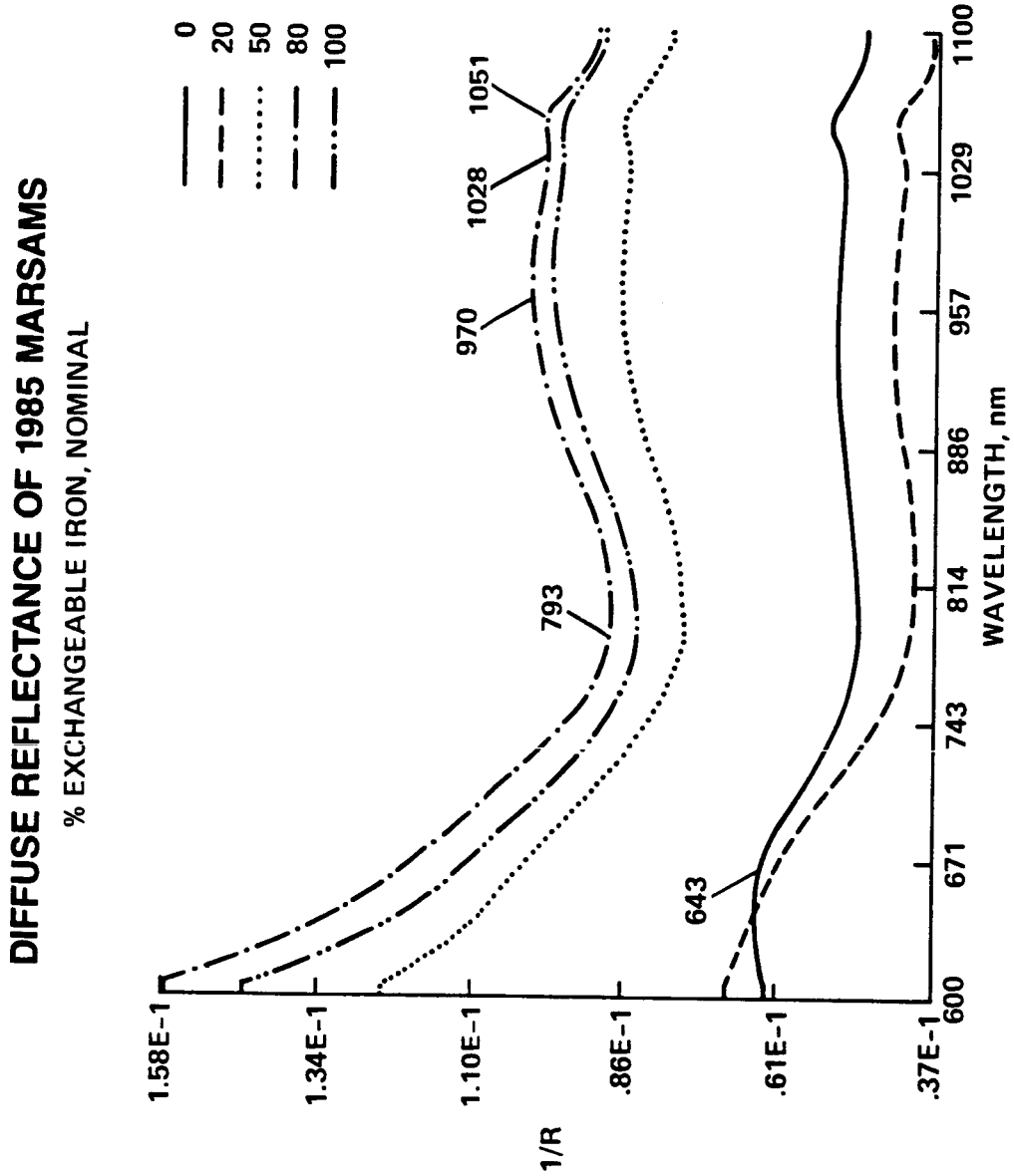
DIFFUSE REFLECTANCE OF 1985 MARSAMS
% EXCHANGEABLE IRON, NOMINAL
0
20
50
80
100
1.58E-1
1.34E-1
1.10E-1
.86E-1
.61E-1
.37E-1
1/R
600
671
743
814
886
957
1029
1100
WAVELENGTH, nm
643
793
970
1028
1051

Figure 6a

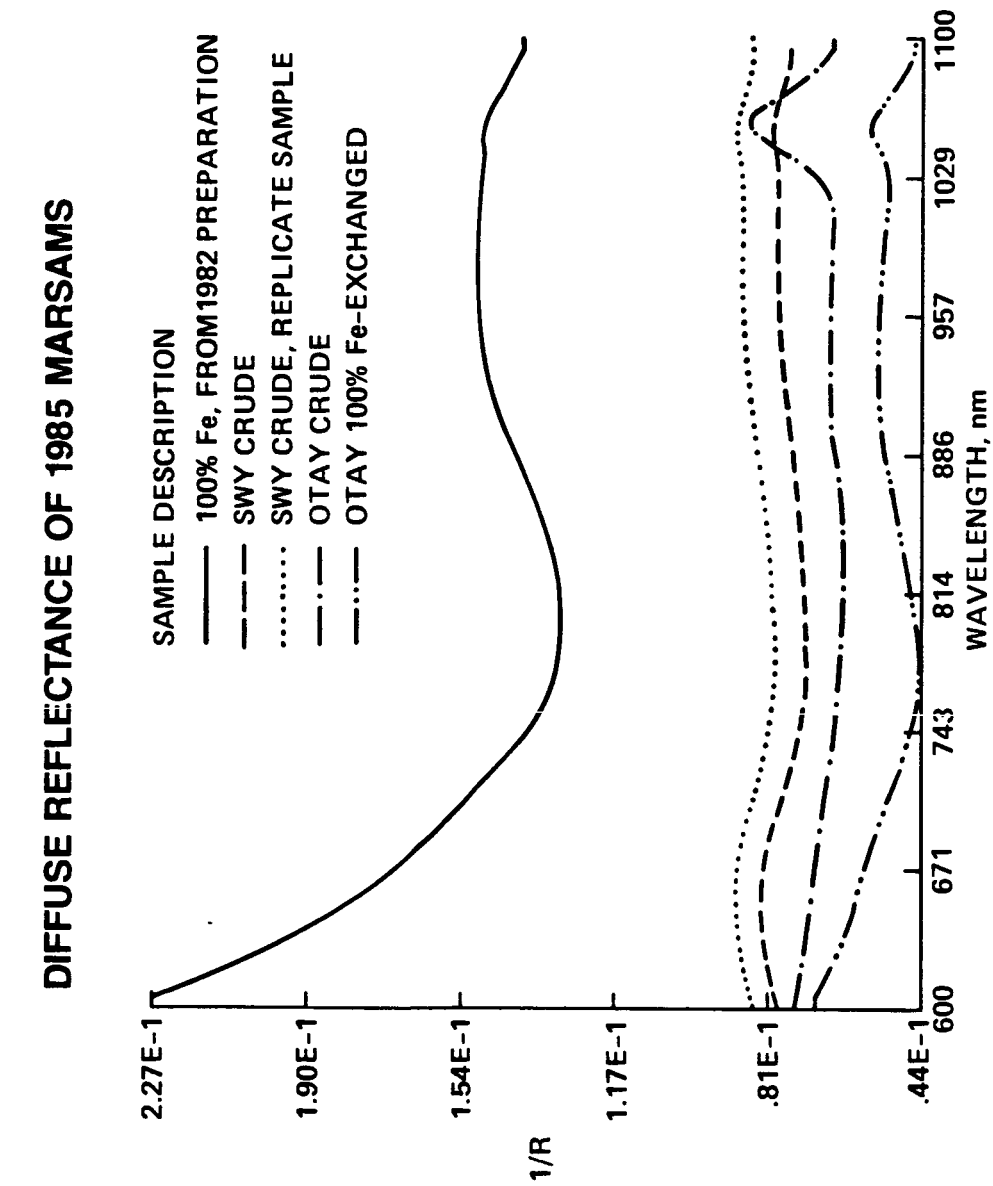
DIFFUSE REFLECTANCE OF 1985 MARSAMS
SAMPLE DESCRIPTION
100% Fe, FROM1982 PREPARATION
SWY CRUDE
SWY CRUDE, REPLICATE SAMPLE
OTAY CRUDE
OTAY 100% Fe-EXCHANGED
2.27E-1
1.90E-1
1.54E-1
1.17E-1
.81E-1
.44E-1
1/R
600
671
743
814
886
957
1029
1100
WAVELENGTH, nm

Figure 6b

The Pacific Scientific (PSCO) simple regression analysis was applied to the 1/R data itself and to the 1st and 2nd derivative data using the total iron determined by XRF as constituent data. A comparison between the analytical values for iron are compared with those calculated from the simple regression of the optical data in **Table 2.** The goodness of the fit, as indicated by the differences between the analytical and calculated iron concentrations, is improved by use of the 1st derivative data and further still by use of the 2nd derivative data. This improvement was expected from the fact that baseline offsets are clearly apparent in the 1/R data.

The wavelength dependence of the simple correlations between reflectance and analytical data derived from linear regressions of the total iron with 1/R and its first and second derivatives at each wavelength are shown in **Figure 7** for the full set of 1985 Marsams. The same data is shown in a different presentation in **Figures 8-10** in comparison with that acquired using sample subsets where the samples were more similar in characteristics. The full set included five materials all of which were produced from the same parent SWY material using the acid pre-treatment and ion-exchange refinement technique of Banin and variably-cation exchanged with pre-selected ratios of iron and calcium, two samples of crude SWy-1, one sample of 100% Fe material produced in 1982 and two clays from a different parent montmorillonite, a crude Otay and its 100% Fe-cation exchanged form.

The correlation with total iron from the 1/R data is moderate, but not striking throughout the spectral range. The mediocrity of the correlation is taken to illustrate the non-homogeneity of the samples included in the full set. There are many species of iron represented in this small sample set, as will be discussed further in the discussion of the correlations obtained using various more homogeneous subsets.

Table 2

COMPARISON BETWEEN ANALYTICAL TOTAL IRON AND TOTAL IRON CALCULATED BY LINEAR REGRESSION OF OPTICAL DATA AS A FUNCTION OF IRON FOR MarSAM SAMPLES 1–5

SAMPLE #	ANALYTICAL IRON CONTENT	MATHEMATICS TRANSFORM OF OPTICAL DATA USED FOR LINEAR REGRESSION ANALYSIS		
		I/R	1ST DERIVATIVE I/R	2ND DERIVATIVE I/R
		ANALYTICAL–CALCULATED	ANALYTICAL–CALCULATED	ANALYTICAL–CALCULATED
1	3.870	0.046	-0.029	-0.020
2	4.111	-0.053	-0.010	+0.011
3	5.210	0.105	0.122	+0.022
4	5.960	0.159	-0.001	-0.009
5	6.080	-0.256	-0.082	-0.007
STANDARD ERROR	–	0.159	0.087	0.020

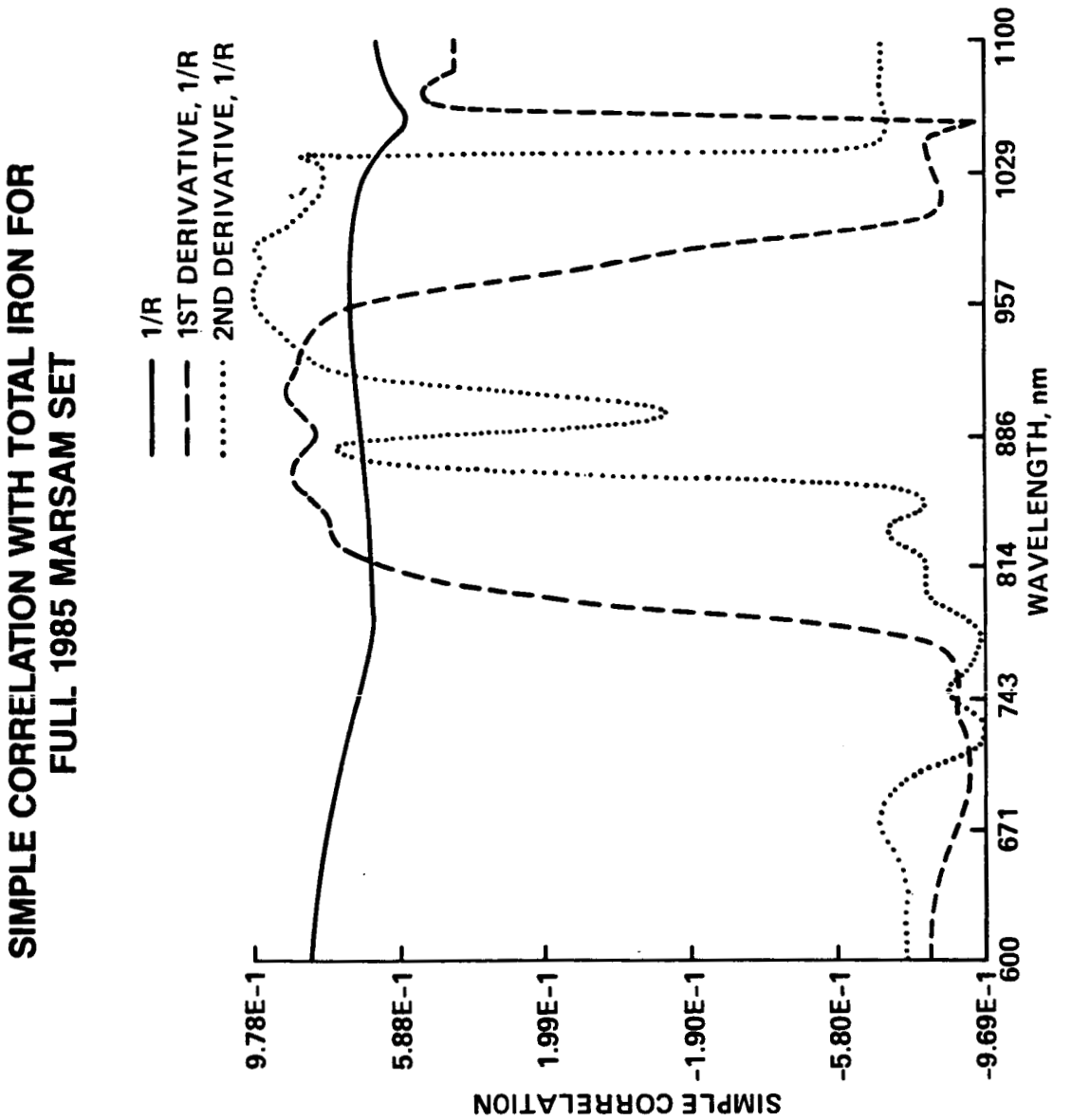
SIMPLE CORRELATION WITH TOTAL IRON FOR
FULL 1985 MARSAM SET
1/R
1ST DERIVATIVE, 1/R
2ND DERIVATIVE, 1/R
9.78E-1
5.88E-1
1.99E-1
-1.90E-1
-5.80E-1
-9.69E-1
SIMPLE CORRELATION
600
671
743
814
886
957
1029
1100
WAVELENGTH, nm

Figure 7

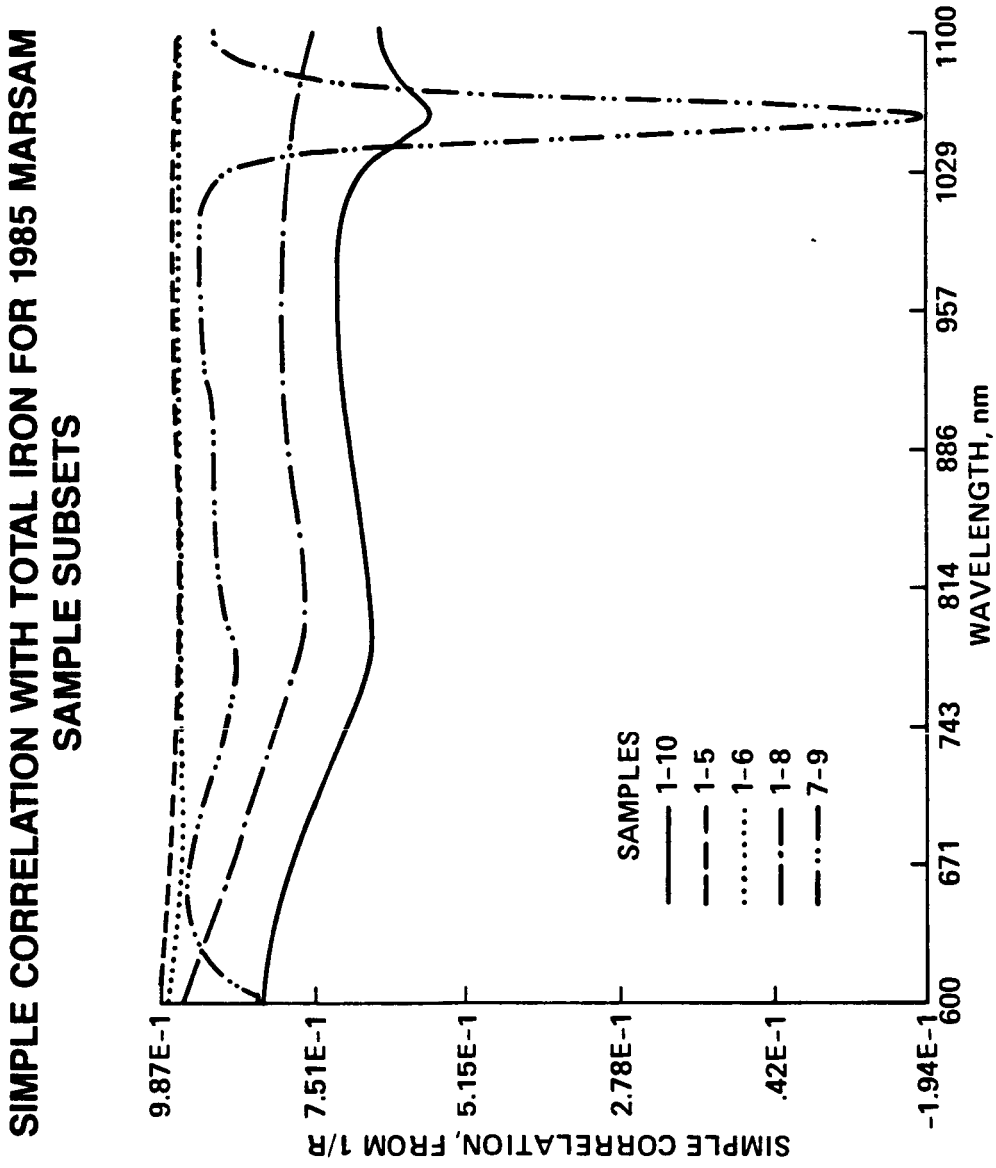
SIMPLE CORRELATION WITH TOTAL IRON FOR 1985 MARSAM
SAMPLE SUBSETS
SIMPLE CORRELATION, FROM 1/R
9.87E-1
7.51E-1
5.15E-1
2.78E-1
.42E-1
-1.94E-1
600
671
743
814
886
957
1029
1100
WAVELENGTH, nm
SAMPLES
1-10
1-5
1-6
1-8
7-9

Figure 8a

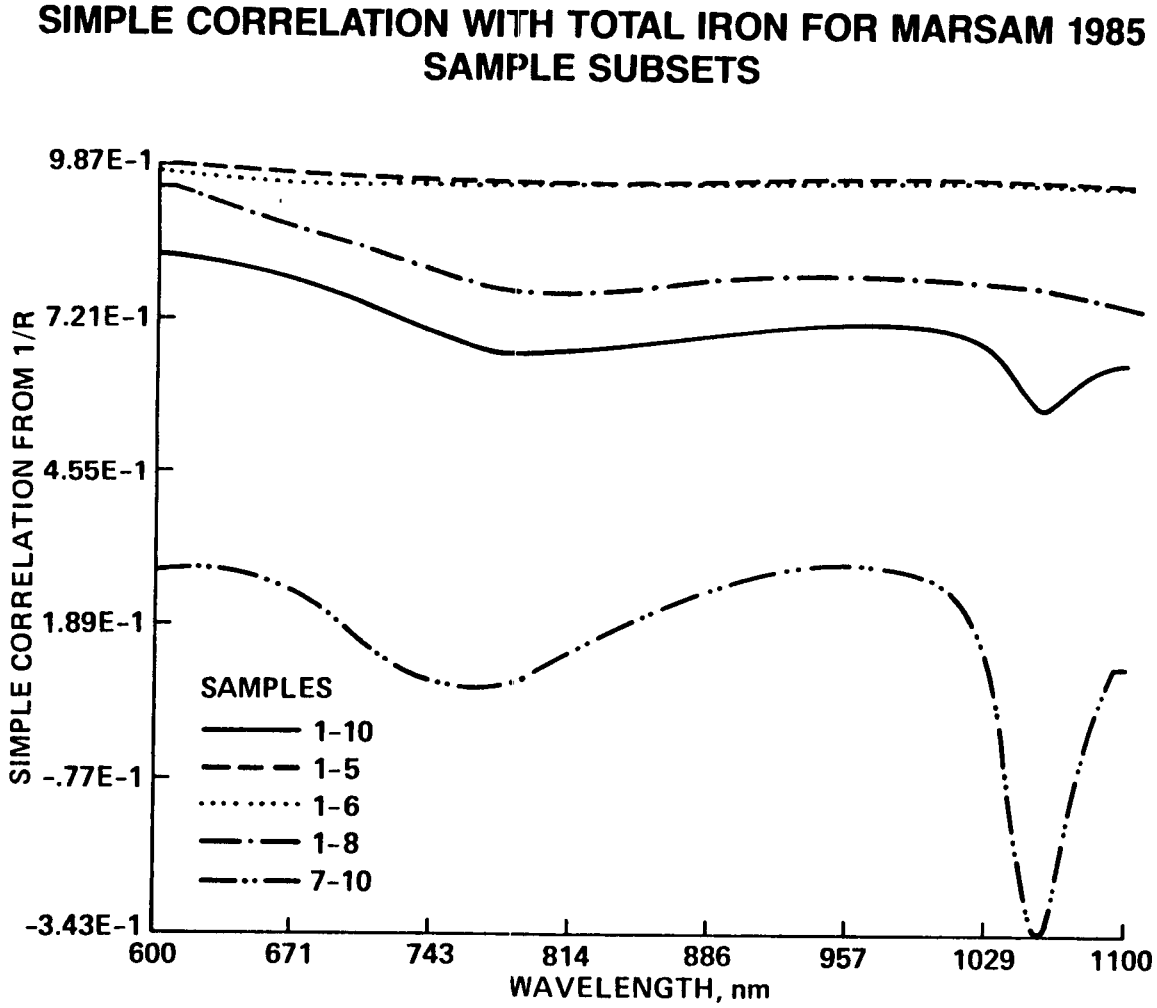
SIMPLE CORRELATION WITH TOTAL IRON FOR MARSAM 1985
SAMPLE SUBSETS
9.87E-1
7.21E-1
4.55E-1
1.89E-1
-.77E-1
-3.43E-1
SIMPLE CORRELATION FROM 1/R
SAMPLES
1-10
1-5
1-6
1-8
7-10
600
671
743
814
886
957
1029
1100
WAVELENGTH, nm

Figure 8b

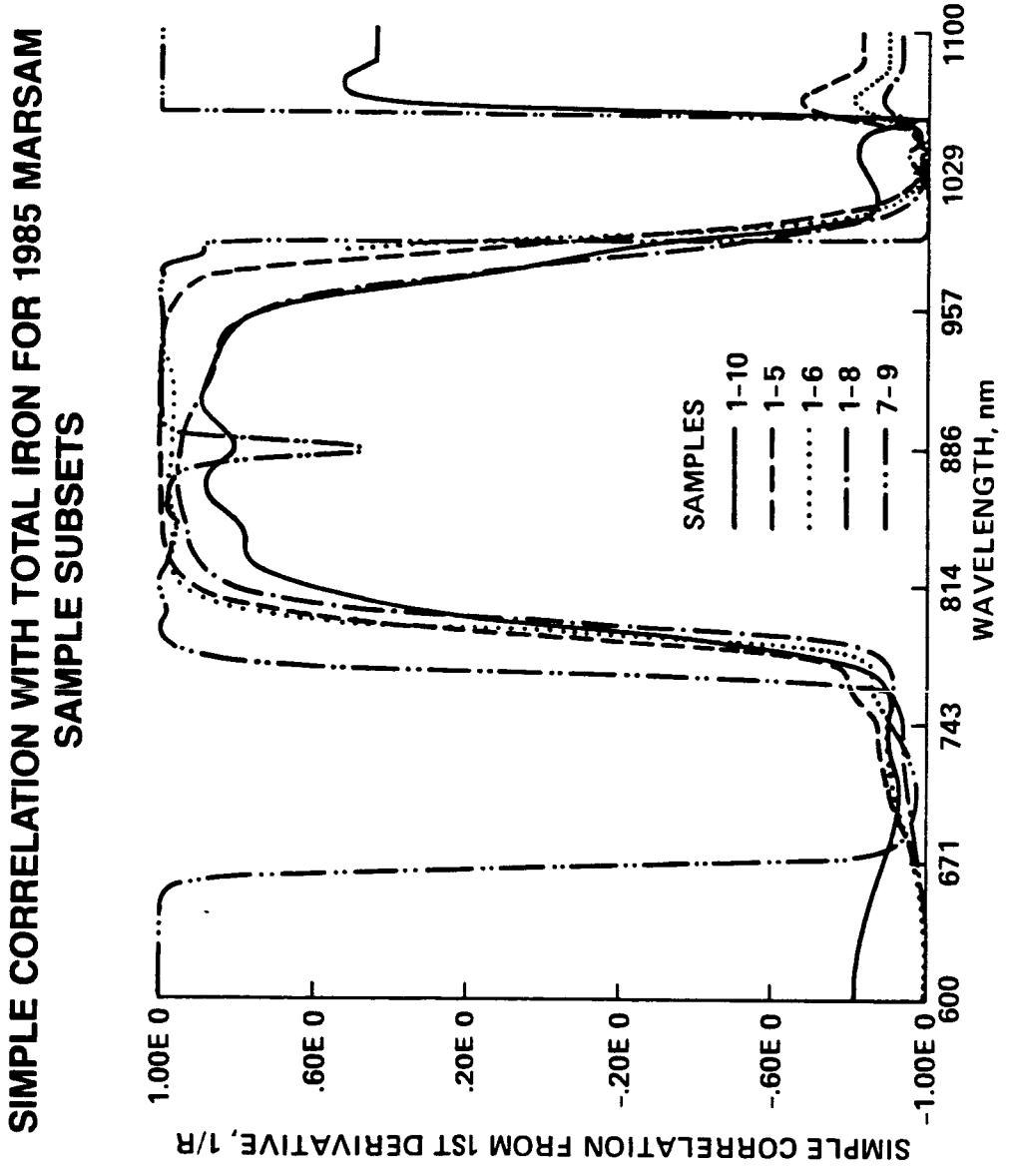
SIMPLE CORRELATION WITH TOTAL IRON FOR 1985 MARSAM
SAMPLE SUBSETS
SIMPLE CORRELATION FROM 1ST DERIVATIVE, 1/R
1.00E 0
.60E 0
.20E 0
-.20E 0
-.60E 0
-1.00E 0
600
671
743
814
886
957
1029
1100
WAVELENGTH, nm
SAMPLES
1-10
1-5
1-6
1-8
7-9

Figure 9a

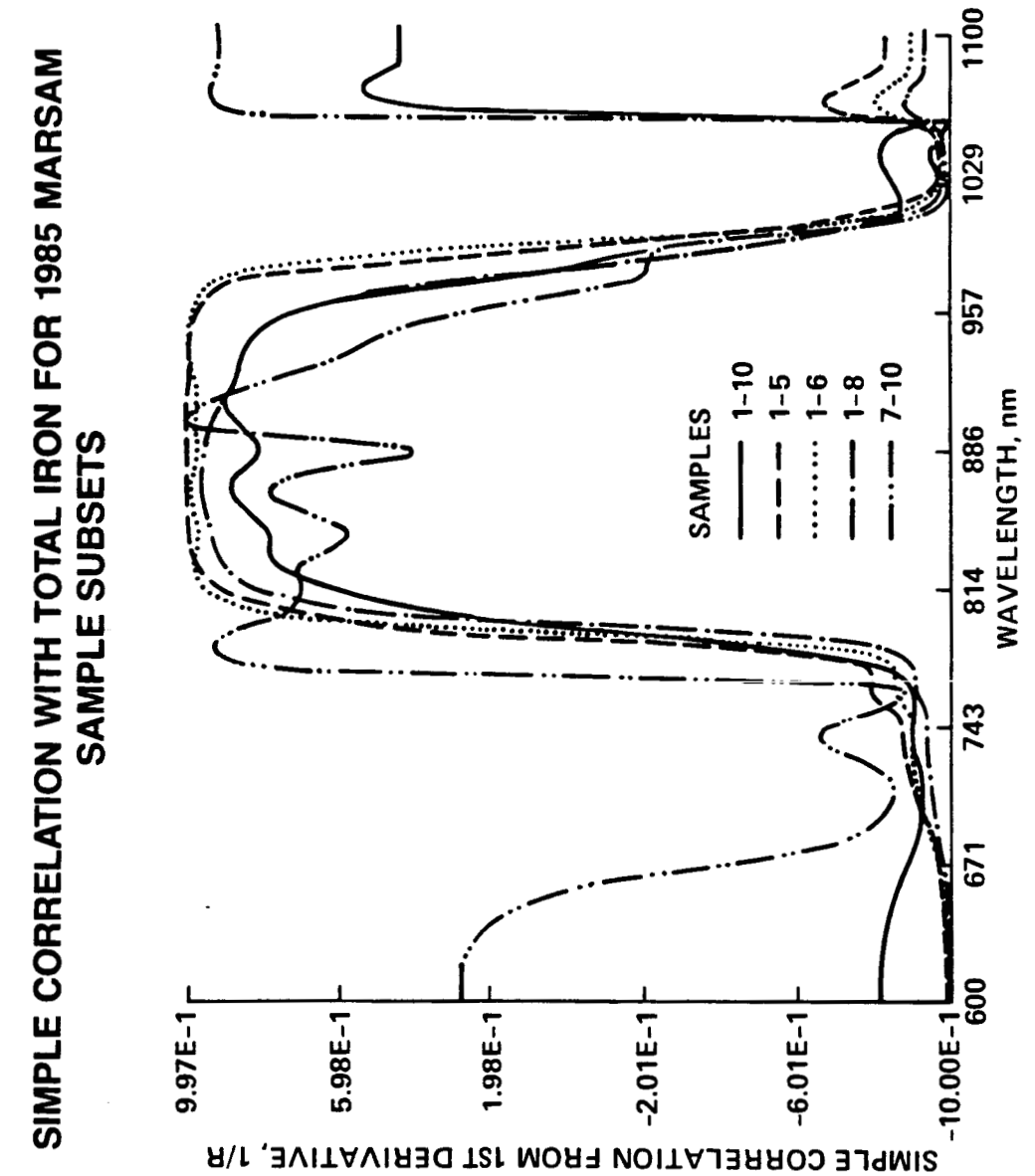
SIMPLE CORRELATION WITH TOTAL IRON FOR 1985 MARSAM
SAMPLE SUBSETS
SIMPLE CORRELATION FROM 1ST DERIVATIVE, 1/R
9.97E-1
5.98E-1
1.98E-1
-2.01E-1
-6.01E-1
-10.00E-1
600
671
743
814
886
957
1029
1100
WAVELENGTH, nm
SAMPLES
1-10
1-5
1-6
1-8
7-10

Figure 9b

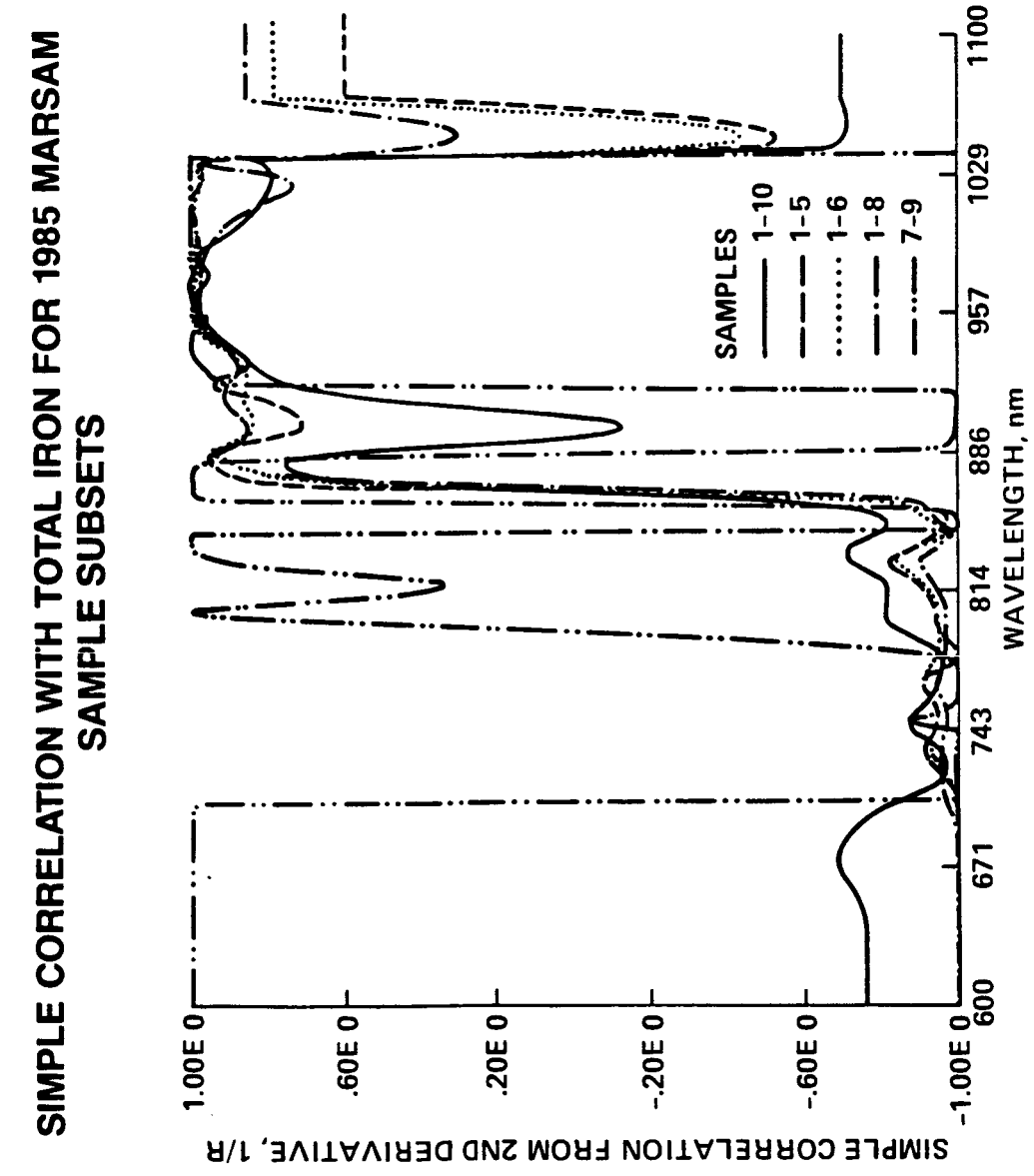
SIMPLE CORRELATION WITH TOTAL IRON FOR 1985 MARSAM SAMPLE SUBSETS
SIMPLE CORRELATION FROM 2ND DERIVATIVE, 1/R
1.00E 0
.60E 0
.20E 0
-.20E 0
-.60E 0
-1.00E 0
600
671
743
814
886
957
1029
1100
WAVELENGTH, nm
SAMPLES
1-10
1-5
1-6
1-8
7-9

Figure 10a

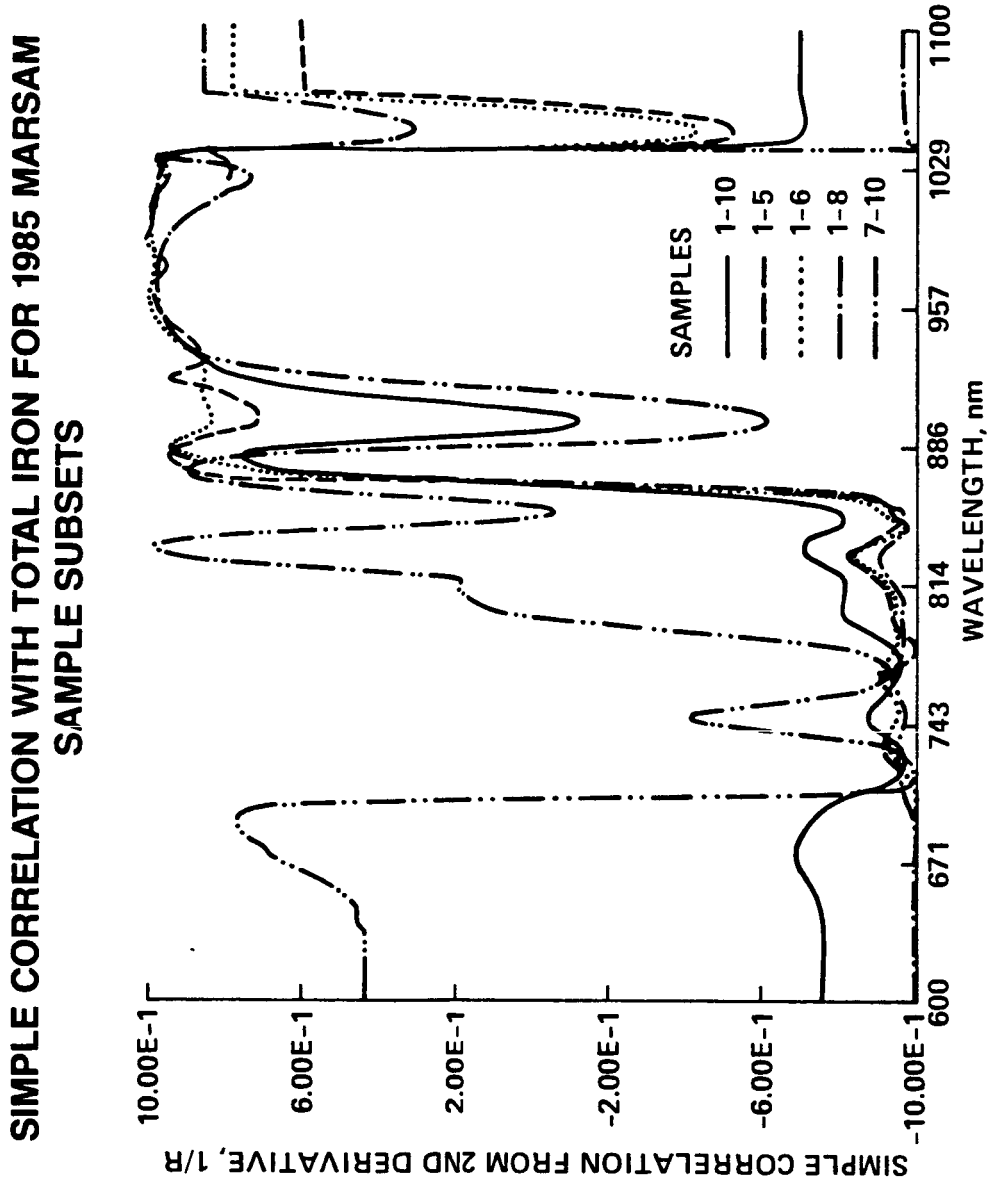
SIMPLE CORRELATION WITH TOTAL IRON FOR 1985 MARSAM
SAMPLE SUBSETS
SIMPLE CORRELATION FROM 2ND DERIVATIVE, 1/R
10.00E-1
6.00E-1
2.00E-1
-2.00E-1
-6.00E-1
-10.00E-1
600
671
743
814
886
957
1029
1100
WAVELENGTH, nm
SAMPLES
1-10
1-5
1-6
1-8
7-10

Figure 10b

The wavelength non-specificity of the correlation with 1/R is not surprising, in view of the breadth both of the charge transfer band, which is known to peak only in the ultraviolet, and that of the band at 970. It is possible, even likely, that other iron-associated transitions may also be underlying these two apparent ones, as other analyses of the iron have shown surface iron to exist in both ferrous and ferric oxidation states and the samples are known to contain structural, as well as surface iron. The derivative spectra produce a narrower range of wavelengths considered to be valuable for the correlation, but the correlations within these ranges are better, as expected, because of removal of the substantial baseline offsets.

The wavelengths chosen by the computer as best correlated with the iron make good sense with respect to the visual assessment of the data. They lie on the charge transfer tail, most conspicuously at 600 nm for the 1/R data and on the 970 peak, though on the rising or falling portions of it, rather than exactly at the maximum. Particularly in the case of the 1st derivative data, the error would be very large at the peak itself, where the curve passes through 0. It is to be expected that the best fit might not fall on the peak itself, for this reason and also because underlying absorptions may affect which region is most responsive to the iron.

In order to point out some more subtle trends, the regressions were run on selected subsets of this initial set of 10 materials, chosen to group them by increasing dissimilarity of parentage or chemical treatment. Correlation functions of the multiple regressions of iron vs. 1/R for these subsets are shown in **Figure 8 a-b - 10 a-b.** The data has been condensed in **Tables 3 -5.** For these tables, several key wavelengths were selected from the multiple regression curves of the 1/R data and its first and second derivatives. The wavelengths selected for comparison are 600 nm, the shortest of the wavelengths examined, because the contribution from the c.t. tail will be maximal here; 643, where the

CORRELATION BETWEEN TOTAL IRON AND OPTICAL DATA (I/R) AT SEVERAL KEY WAVELENGTHS

SAMPLE SUBSET	MAXIMUM VALUE OF CORRELATION (AUTO SEARCH)		WAVELENGTH					
			C-T REGION			D-D REGION		
			600	643	793	970	1028	1051
	λ	CORRELATION	(INITIAL)	("Ca" MAX.)	(MINIMUM)	(BROAD PEAK)	TROUGH	NARROW PEAK
1–5 SWY 1985 ALL TREATED VARIABLE IRON	600	0.987	0.987	0.980	0.959	0.967	0.965	0.962
1–6 SWY 1985, AS ABOVE WITH 100% Fe PREPARED IN 1982	600	0.975	0.975	0.962	0.954	0.959	0.958	0.956
1–8 1–6 AS ABOVE WITH 2 REPLICATE SAMPLES OF CRUDE SWY	600	0.949	0.949	0.909	0.767	0.798	0.786	0.780
7–9 2 CRUDE SWY + 1 CRUDE OTAY	664	0.946	0.838	0.941	0.879	0.925	0.889	0.058
7–10 2 CRUDE SWY + 1 CRUDE OTAY + 1 OTAY 100% Fe	1057	-0.343	0.283	0.279	0.101	0.296	0.150	-0.287
1–10 FULL SAMPLE SET	600	0.830	0.830	0.811	0.664	0.713	0.680	0.584

Table 3

CORRELATION BETWEEN TOTAL IRON AND OPTICAL DATA (1ST DERIVATIVE OF I/R) AT SEVERAL KEY WAVELENGTHS

SAMPLE SUBSET	MAXIMUM VALUE OF CORRELATION (AUTO SEARCH)		WAVELENGTH					
			C-T REGION			D-D REGION		
			600	643	793	970	1028	1051
	λ	CORRELATION	(INITIAL)	("Ca" MAX.)	(MINIMUM)	(BROAD PEAK)	TROUGH	NARROW PEAK
1–5 SWY 1985 ALL TREATED VARIABLE IRON	900	0.997	-0.991	-0.988	0.393	0.914	-0.978	-0.930
1–6 SWY 1985, AS ABOVE WITH 100% Fe PREPARED IN 1982	600	-0.994	-0.994	-0.991	0.298	0.943	-0.987	-0.957
1–8 1–6 AS ABOVE WITH 2 REPLICATE SAMPLES OF CRUDE SWY	600	-0.996	-0.996	-0.995	-0.308	0.427	-0.977	-0.973
7–9 2 CRUDE SWY + 1 CRUDE OTAY	1035	-1.000	-0.999+	0.998	0.999	0.997	-1.000	-0.999+
7–10 2 CRUDE SWY + 1 CRUDE OTAY + 1 OTAY 100% Fe	1023	-1.000	0.283	0.171	0.859	-0.0707	-0.997	-0.993
1–10 FULL SAMPLE SET	1056	-0.956	-0.816	-0.841	-0.0517	0.362	0.837	-0.869

Table 4

CORRELATION BETWEEN TOTAL IRON AND OPTICAL DATA (2ND DERIVATIVE OF I/R) AT SEVERAL KEY WAVELENGTHS

SAMPLE SUBSET	MAXIMUM VALUE OF CORRELATION (AUTO SEARCH)		WAVELENGTH					
			C-T REGION			D-D REGION		
			600	643	793	970	1028	1051
	λ	CORRELATION	(INITIAL)	("Ca" MAX.)	(MINIMUM)	(BROAD PEAK)	TROUGH	NARROW PEAK
1–5 SWY 1985 ALL TREATED VARIABLE IRON	1000	1.000	-0.996	-0.998	-0.945	0.985	0.944	-0.492
1–6 SWY 1985, AS ABOVE WITH 100% Fe PREPARED IN 1982	693	-1.000	-0.997	-0.998	-0.947	0.991	0.966	-0.408
1–8 1–6 AS ABOVE WITH 2 REPLICATE SAMPLES OF CRUDE SWY	636	-0.997	-0.997	-0.997	-0.960	0.973	0.763	0.308
7–9 2 CRUDE SWY + 1 CRUDE OTAY	848	-1.000	0.999+	0.999	0.0853	0.999	0.999+	-1.000
7–10 2 CRUDE SWY + 1 CRUDE OTAY + 1 OTAY 100% Fe	989	1.000	0.436	0.456	-0.238	0.987	0.963	-0.967
1–10 FULL SAMPLE SET	963	0.978	-0.754	0.753	-0.855	0.968	0.786	-0.709

Table 5

low iron SWY samples show a maximum and the Otay ones a clearly discernable inflection point, the assignment of which is not known; 793, a region of minimum absorption, thus expected to be a region which is relatively constant within a sample set of homogeneous parentage, but which might be indicative of structural variability between dissimilar starting materials; 970, the broader peak which appears to increase with increasing iron; 1051, the narrower peak, which does not appear to increase with increasing iron; and 1028, the trough between these two peaks, which is susceptible to being filled in if either of the two peaks increases in intensity.

Discussion of Results

Admittedly, our full sample set of ten members is small, and the subsets are miniscule, in a statistical sense. However, the materials are of sufficient and known structural similarity that the beginnings of clear predictors of the behavior of larger data sets can be discerned and discussed, in order to illustrate the potential and some of the limitations of this method in more general terms.

Samples 1-5, previously discussed, are the most like each other. Also, the analytical data given for them is most indicative of differences between them in the surface iron, as the structural component is common for them all and they have been cleansed of surface iron oxides, unlike the crude material. The correlation with iron is excellent. In set 1-6, we add the 100% iron sample prepared in 1982. In set 1-8 we include the two replicate samples of the parent crude SWy montmorillonite. In set 7-9 we compare the crude SWy with the crude Otay. These clays are known to have significantly different contents of structural iron - as evidenced by the large difference in their respective iron analyses. The distribution of the iron between structural and surface oxide coatings is not known, but some indication of this can be surmised for the SWY material from the fact that its acid-treated 100% Ca derivative has the same iron content as the crude. Apparently

most of the iron in crude SWy is in the clay structure itself. If a similar distribution is assumed for the Otay, the fact that the change from the crude to the 100% Fe material produces a 2.4% increase vs. the 3.2% increase for the SWy clay, would indicate that the cation-exchange capacity of the Otay would be 2/3 that of the SWy and thus the 100% form would have 2/3 the surface iron of the SWy. Unfortunately, crosschecks of the accuracy of the analytical data are not available to us at this time, so the assumption must be made that it is valid, in addition to the assumptions just made about the distribution of the iron.

The truly excellent correlation with iron in group 1-5 where the samples were all prepared in 1985, of homogeneous parentage and only one substituent is being varied is not significantly diminished by adding the similar material produced in 1982. It can be inferred from this "robustness" of the fit to additions of a material prepared earlier that the method by which the samples is prepared produces a product which is stable over lengthy periods of time - reassuring, to say the least. Adding in the parent material did force more discrimination of the wavelengths chosen for the fit, but did not cause loss of recognition of the similarity between the materials. That there is a significant difference between the crude and treated materials, evidenced by the preferred wavelengths for good correlation and in the magnitude of the correlation itself, can mean one or a combination of several things. Extraneous mineral constituents would have been removed by the pre-purification; the texture of the material may have been altered; there may have been some low-level alteration of the structure of the material itself.

In **Figure 11**, a tree is shown which indicates the diversity of the possible species of iron in these materials. Given that the absorption maxima and extinction coefficients for these various species are expected to be different from each other, depending on the degree of difference between the ligand configurations of iron in the various sites, it is not

PARTIAL IRON SPECIATION IN IRON BEARING CLAYS

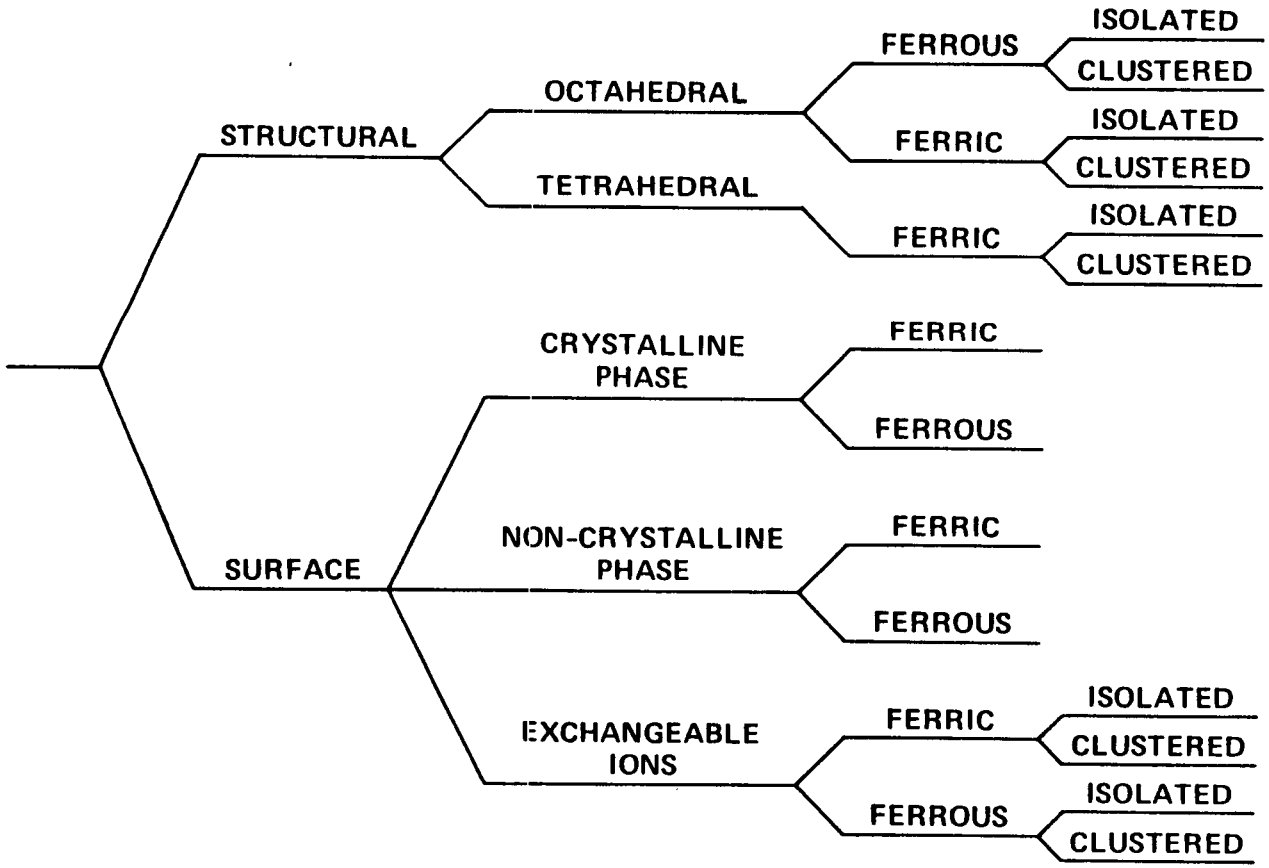

Figure 11

to be expected that perfect correlations, perhaps even meaningful ones, can be derived from data that does not speciate the iron into its different environments - both qualitatively and quantitatively. With this fresh consideration clearly in mind, the remaining sub-groups, 7-9, 7-10, and the full set, all of which contain materials selected from different parents, can be discussed in relationship to the more homogeneous group represented by samples 1-8.

The subset 7-9, where dissimilar parent materials are compared, also gives a good correlation - but for the wrong reasons. The data provided to the computer was for the total iron - no implications as to speciation. As mentioned earlier, the likelihood is that neither the crude SWy nor the Otay contain significant surface iron. Therefore, the comparison being done in this subset is between different amounts of structural iron. It should be noted that for all subsets containing the Otay materials the wavelengths of maximum correlation are different from those subsets containing only SWy materials. Even though there are several favored wavelengths for the SWy-only subsets, the correlation differences between these are small and all of these favored wavelengths are clearly associated with either the charge transfer tail or the 970 broad peak. Neither of these wavelengths was selected for the Otay-containing subsets, as would be expected from the fact that including Otay samples introduces a new variable. In spite of the smallness of the sample sets, it seems highly likely that these observations are valid and reflective of the real differences in the structural iron in the two clays, but, of course, inaccurate representations of either surface or total iron.

All signs of pattern-recognition are obviated in the 1/R data of subset 7-10. The situation is similar, but not quite so profound in the 2nd derivative data. The first derivative data, interestingly, still shows good correlation. Consideration of whether this correlation seems even possibly valid, given what we know, or can surmise, about the

iron transitions and species involved seems premature. It can be rationalized, but proof of such rationalization can not acquired from the present data set, so will not be further discussed.

The full set shows correlations which probably are actual, but which are significantly deteriorated from those seen from the groups which have common parents. It would be expected that provision of speciated iron data would restore the correlation significantly. Using this limited data set, the strength of the correlations observed appears well-connected with the what is known about the abundance and speciation of iron in these materials.

General Comments on NIRA Application Methods for Iron-bearing Clays

Two risks must be balanced against each other, if correct interpretation of the data is to be achieved as the sample set is enlarged. Given that a regression analysis has been performed on the data at each of 500 wavelengths and there are only 5-10 samples in our initial analysis set, there remains some significant probability that a correlation may be produced which is spurious. Such spurious correlations can be rejected with increasing confidence either by associating the analytical wavelength with a spectral feature of distinctive and/or of known assignment, of which the concentrations of the species producing it can be independently and accurately confirmed, or by enlarging the sample set.

As the sample set is enlarged, coincidental correlations will be easier to eliminate, but valid ones may be lost, as well, because the diversity of the samples is increased. For instance, the 970 feature of the SWY clays appears shifted to shorter wavelengths in the Otay clay. Whether a compromise wavelength will be able to be found which recognizes this useful feature, even though it may not coincide with the peak of the transition for either of the individual clays, is an imponderable at this point.

Responsiveness of the spectra to controlled variation of a given constituent are most easily discerned by visual inspection of the 1/R data itself. But, as can be clearly seen in our spectra, quantitative analysis of the 1/R data may compromised either by the presence of the baseline offsets and sloping baselines, which are unavoidable consequences of the sensitivity of reflectance data to orientational and particle geometrical effects, or by species diversity which compromises the choice of an analytical wavelength which is sensitive to variation of the constituent under consideration for a diverse group of related samples. There are various methods which can be used to assist in improving quantitation of a given constituent.

It has not been previously mentioned, nor have we yet made use of it, but it should be discussed briefly that additional valuable information is obtainable from the slope of the regression curve in which concentration of the constituent, (ordinate) is plotted versus 1/R, (abcissa). This slope dictates the responsiveness of the optical data to changes in the concentration of the constituent. A steep slope in this curve represents a sub-optimal choice of analytical data, because a large change must be made in the concentration of the analyte in order to produce a significant change in the optical data. (Unfortunately, the terminology used in NIRA is confusing, as the slope of the line previously defined, dubbed "sensitivity", is inversely, rather than directly related to the responsiveness of the optical data to changes in the concentration.) Low responsiveness of 1/R, to changes in concentration, i.e. large slopes, i.e high sensitivity, would be the relationship expected when the absorption of the chromophoric group of interest is superimposed on that of other chromophores, or on a high scattering background.

That there are multiple contributions to the 1/R data obtained at any wavelength in the spectra from complex mixtures, is the reason that the ideal analytical wavelegth so often

departs from that of the spectral feature which is visually the most easily associated with a given constitutent. Between two features of equivalent visual distinctiveness, the more favorable choice for quantitative analysis would be the one less underlain by extraneous absorptions, i.e. the wavelength region demonstrating the lower slope. On the other hand, such a choice might shift the optical analytical wavelength for a large sample set out of the range of responsiveness to that of a very distinctive feature of some subset of interest.

Baseline offsets and slopes can be eliminated by using 1st and 2nd derivative transforms of the 1/R data, thus maximizing the responsiveness of the optical data to changes in the concentration. In this case derivatives allow for partial or complete removal of the absorptions producing the background, thus abstraction of the distinctive feature from a high background. However, use of derivative data does not assist in finding a compromise wavelength when a distinctive transition is shifted by local environmental differences between individual members of a large common class of materials. In finding an appropriate analytical wavelength the sensitivity curves are often of assistance additional to that acquired from use of derivative data.

Beyond doubt, physical "sensibility" is by far the strongest criterion for the choice of a valid analytical wavelength. A "sensible" wavelength is based on theoretical and experimental assignments of the transitions under consideration, for a well-controlled samples set However the optimal wavelength choice for a given constituent of a large, incompletely characterized sample set may or may not lie at the peak wavelength of a known transition determined using the small control set. Many other contributory factors must also be taken into consideration in selecting a wavelength which is a quantitatively, as well as qualitatively, reliable indicator of amount of a known constituent. There are several means by which an analytical wavelength can be selected, the choice of which

will depend on the particular application. Clearly there will always remain some level of subjectivity in optimizing the analytical wavelength for any particular application and much room for reinforcement of an initial choice by the iteration of the regression including terms based on more than one wavelength.

Despite many caveats, the overall conclusion that can be offered at this time from this very incomplete analysis, is that the method looks capable of doing everything we predicted it could. The fineness and the certainty of the discriminations that can be produced from it will, however, depend critically on three important features: 1) The analytical data must be reliable, thus must be confirmed by replication and by producing it using more than one method. 2) In making definitive discriminations between materials which are related by elemental composition, but which have significant structural distinctions, it will be important to provide the computer with information on the distribution of the structural element of interest between dissimilar sites, as well as the overall abundance. Means by which we can extend our knowledge of the various species of iron, one of the most important elemental constituents of our materials and of the Martian soil, will be discussed in the section on Proposed Research. 3) Recognition of each of the distinctive species of an overall major constituent and distinction between those analytical wavelengths which are optimal for individual species as opposed to the over-all abundances can be achieved by the use of fastidiously selected subgroups, in which concentration of the individual species can be independently varied and analytically confirmed.

RELATIONSHIPS BETWEEN STRUCTURAL FEATURES MEASURABLE BY INDEPENDENT SPECTROSCOPIC TECHNIQUES AND ENERGY STORAGE WHICH MAY BE FURTHER EXPLORED USING NIRA.

Relationship Between Surface Iron in Marsams and Thermoluminescence

Coyne and Banin (1986) have sketched the relationship of surface iron and stored energy in the 1982 Marsams as evidenced by the changes in the intensity of the thermoluminescence output from both untreated and gamma-irradiated samples throughout the series of the various iron/calcium exchanged materials. In this study, the electron spin resonance spectra of the materials were also recorded, as a monitor of both surface and structural iron, but no effort was made to quantitate the energy stored as O^- - centers. It was observed that the g = 4 component of the signal, attributable to structural ferric iron (Goodman, 1978) was not affected by the increasing surface iron, but that the g = 2 component, attributable to surface ferric iron, increased steadily, albeit non-linearly, with increasing substitution of Fe for Ca. That these two species of iron have signals which are simply separable using ESR suggests that the ESR intensities might be used as constituent data for NIRA.

It was also noted that there appears to be some non-trivial relationship between the stored energy manifested as thermoluminescence and the amount of surface iron. Both signal intensities tend to saturation as the surface iron exceeds 50% of the cation exchange capacity. Such a relationship is of significance as it implies that, for these materials, structural and surface states may interact to a significant degree, in a manner such that either the energy storage capacity, the residence time or the surface availability of the stored energy is affected by surface iron. Since the surface iron is known to have catalytic properties, such an interaction would imply that, if significant amounts of energy

are stored in these materials, it might have a significant effect on the catalytic activity of the surface. Of interest, in this regard, is that Banin, et al. Appendix A, have noted that the catalytic activity of these clays toward the Simulated Viking Labeled Release experiment also tends to saturation at this same iron content.

Banin et al. also have found that the distribution of the surface iron between exchangeable and acid-extractable fractions stabilizes at >50% surface iron. Below this amount the exchangeable fraction is increasing relative to the acid extractable fraction. We have found that four properties of the system, (extractable vs. exchangeable iron by chemical analysis, ferric iron by E.S.R., stored energy by TL, and reactivity of the surface by surface chemistry) similarly tend toward saturation as nominal exchangeable iron is increased to a value > 50%. Not only, as stated above, do these observations imply the possibility of a non-trivial relationship between stored energy, surface iron and catalytic activity of the surface, but they also imply that one particular component of the surface iron, the exchangeable iron, may play the dominant role in these relationships. Exchangeable iron can be analyzed chemically, so it can be used as constituent data for NIRA. If an analytical wavelength can be determined for exchangeable iron, then these relationships can be further studied using NIRA.

Effect of Interlayer Hydration of Kaolinites on the ESR Signals from Structural Iron and Energy Stored as O^- - Centers

In connection with another NASA grant, "Energetic Contributions of the Mineral Phase to Prebiotic Chemistry on Planetary Surfaces", independent efforts to evaluate the energy storage capacity of 1:1 clays were made using several kaolinites, artificially hydrated kaolinites and natural metahalloysites. Some surprising results were produced that may well bear on the interaction of iron and stored energy in MarSAM's, 2:1 clays, as well. The electron spin resonance (E.S.R.) signal of typical Cornish and Georgia kaolins is shown in **Figure 12a** in comparison with that of the 8.4 A^o hydrated material

EFFECTS OF INTERCALATION OF WATER ON THE ESR OF STRUCTURAL FERRIC IRON IN TWO KAOLINITES

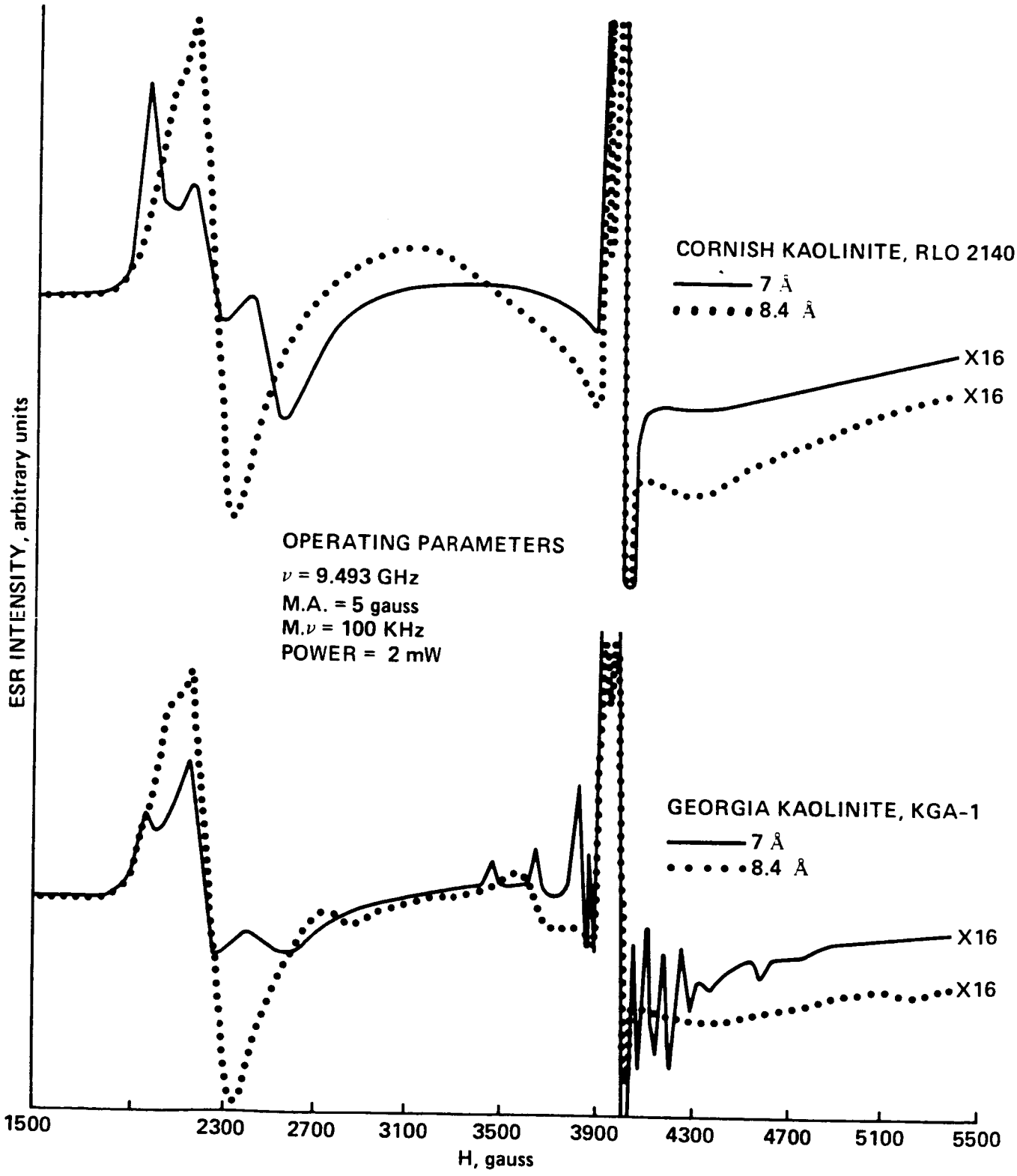

Figure 12a

measured several years after preparation. The O^--center portion of the g = 2 signal is abstracted and scaled for viewing, independent of the contribution from surface iron, in **Figure 12b**. There are three primary regions of interest in these spectra (Hall, 1980). In the vicinity of g = 4, the broad, but structured signal has been attributed to ferric iron in the structure (Jones, et al.,1974); Meads & Malden, 1975). The broad, structureless signal at g = 2 is associated with impurity phases, such as mica, (Meads & Malden, 1975), oxide coatings, (Angel & Vincent, 1978), near-surface structural iron (Herbillon et al., 1976), or (in montmorillonites) as exchangeable cations (Coyne & Banin, 1986). The narrow, structured, signal centered around g = 2 is associated with trapped separated charge pairs near the isomorphically substituted sites, i.e. O^--centers (Angel & Hall,1973; Meads & Malden, 1975; Angel, et al., 1974, 1976, 1977). The analysis of this trapped hole signal into its several tetrahedral and octahedral components has been reported by Angel & Hall (1973) and Meads & Malden, (1975). The E.S.R. signals from two typical, but heavily iron-bearing halloysites, Te Puke and Opotiki and that of an atypical halloysite Matauri Bay in **Figure 13.**

There are two noticeable differences between the kaolinite and the typical halloysite spectra. The structural iron signal at g = 4 is structured in the kaolinites and featureless in the halloysites. The degree of structure of this g = 4 iron signal in kaolinites has been related to the degree of crystallinity of kaolinites - the more crystalline, the more structured and symmetrical the signal (Angel and Hall, 1973; Jones et al. 1974; Meads and Malden, 1975; Mestdagh, et al., 1978). The other observation is that the narrow signal at g = 2, associated with stored energy, is considerably more weak in the halloysites than it is in either the Georgia or the Cornish kaolinites. The degree of surface iron, evidenced by the broad signal centered about g = 2, is variable in both kaolinites and halloysites.

EFFECTS OF INTERCALATION OF WATER ON THE ESR OF O^- - CENTERS IN TWO KAOLINITES

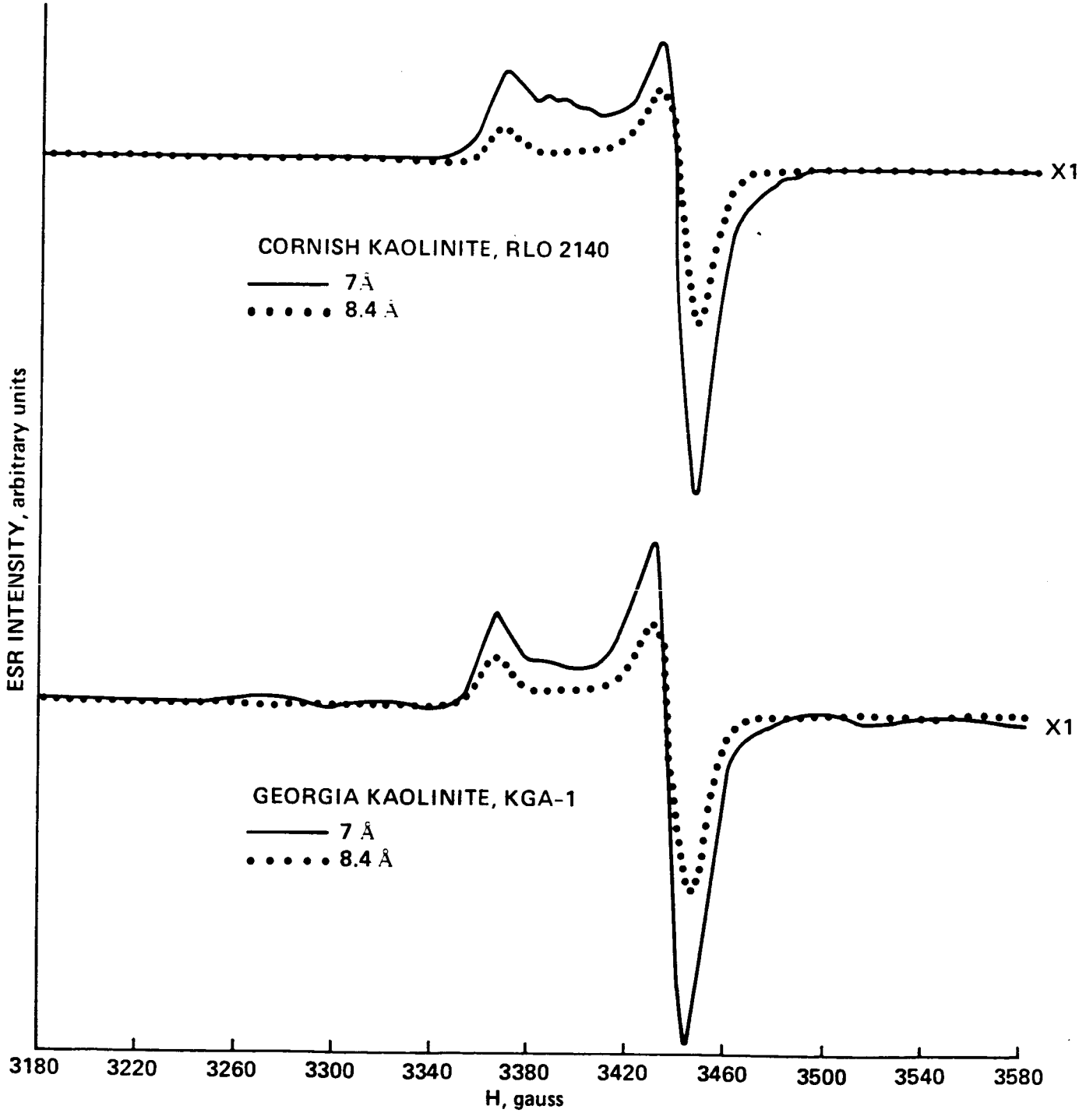

Figure 12b

In addition to the qualitative differences in the spectra of the kaolinites and metahalloysites is an interesting time-dependent phenomenon in the 8.4Å hydrated kaolinite. Immediately after preparation, the ESR signals from the 8.4 Å materials were unaltered from those of the parent 7Å material. The E.S.R. signals of aged 8.4 Å hydrated kaolinites resemble more those of typical halloysites than they do those of the parent kaolinite, in both the loss of structure in the g = 4 signal and in the diminution of the O^- - center signal. The c- spacing determined from the X-ray diffraction spectra of these aged 8.4 A^o materials has not measurably altered over this same time interval. Measures of increased disorder have not been undertaken at this point.

A capacity to emit light upon dehydration has been shown to be a general feature of kaolinites. This light-emitting capacity was equivalent in the freshly prepared 8.4Å material to that of the parent kaolinite for both the Georgia and the Cornish materials. However the capacity was lost over time from the aged materials, although no change was observed in the c-spacing determined by X-ray diffraction over this period of time. The loss of the luminescence capacity paralleled that of the loss in signal intensity in the ESR.

On the basis of the mutuality of the effects of pre-heating and pre-gamma irradiation on the ESR at g = 2 and luminescence intensities (Coyne, et al, 1981, Coyne, 1985) dehydration-induced luminescence has been shown also to be associated with the intensity of that portion of the O^- - center signal which can be ascribed to holes trapped in the tetrahedral layer. On this basis it is to be expected conditions decreasing the O^- - center population in 8.4Å hydrates would be expected also to diminish the luminescence capacity. This further evidence for covariance between the ESR signal of O^--centers and luminescence intensities in kaolinites can be seen as additional confirmation of the previously postulated inter-relationship. Dehydration-induced luminescence has not

EFFECTS OF REMOVAL OF SURFACE IRON ON THE ESR SPECTRA OF THREE NATURAL METHAHALLOYSITES

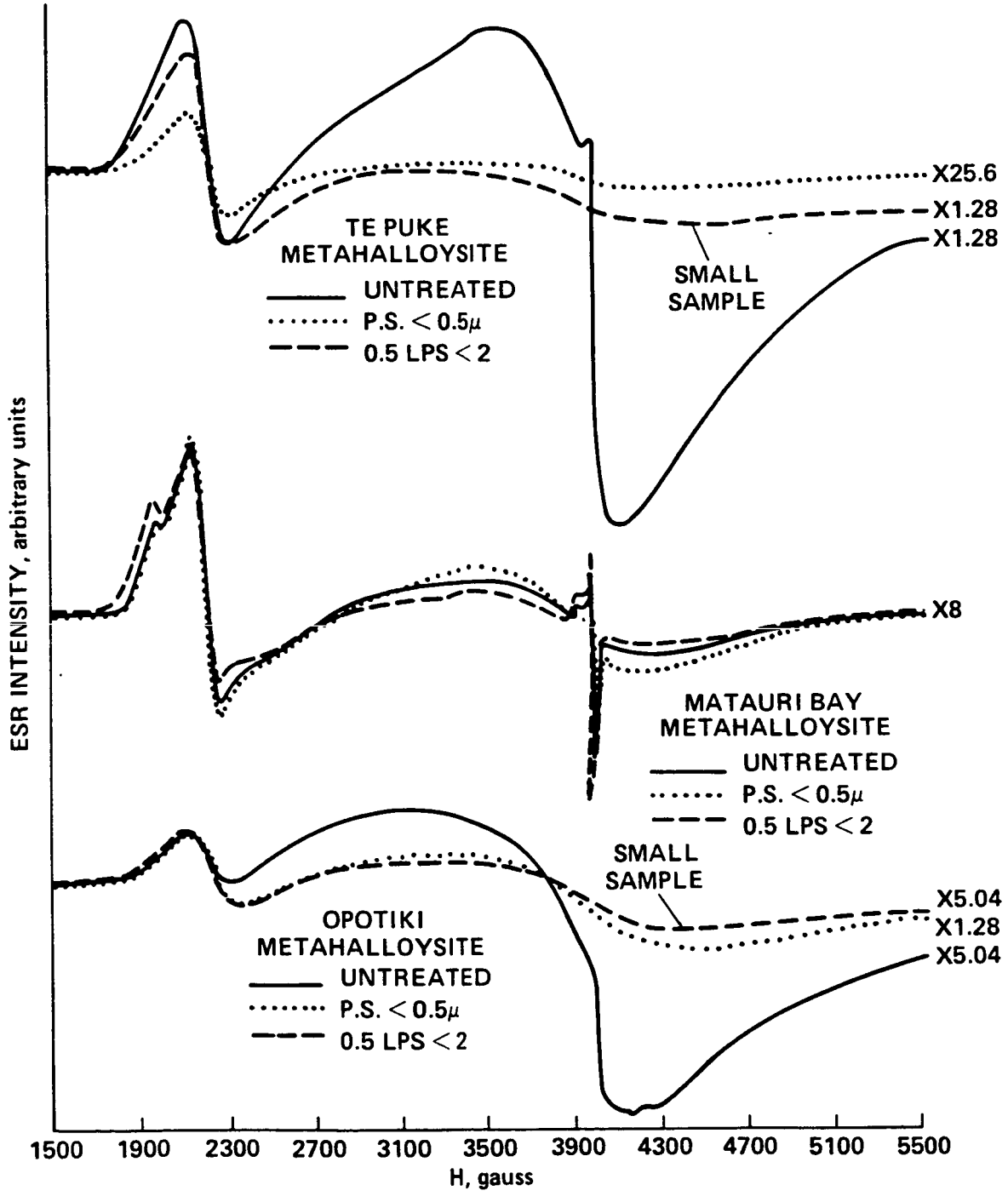

Figure 13

been seen in montmorillonites, a fact which may now possibly be related to the structural and energetic changes that occur as the consequence of the interlayer hydration.

The structural alteration which produces the time-dependent changes in the E.S.R. signals attributable both to structural iron and O^--centers and the intensity of dehydration-induced luminescence is expansion of the interlayer space by water, a surface entity. Expansion would, of course, place more of the bulk material in juxtaposition with the environmental interface. We have not proved that these covarying changes in the molecular environment of structural iron and the content of energy stored as O^--centers are interdependent on each other, only that they mutually are temporally associated with the intercalation history. Still there is reason to believe that the covariances between these three key structural features may not be coincidental, but implicative of interrelationships between a key surface property, interlayer hydration and two constituents, structural iron and O^--centers, of the interior of the crystal.

Interlayer expansion, intercalation, swelling, hydration, however it is designated, of a kaolinite brings it into a state in which it is much more structurally comparable to montmorillonites, thus, MarSAMs. The E.S.R. signal attributable to structural iron from the MarSAMs resembles that of the hydrated, rather than the collapsed kaolinites, a fact perhaps connected to the proximity of these crystal iron centers to the interlayer. In spite of the fact that expanded kaolinites still have two types of external surfaces, and montmorillonites only one, it appears that there may be some significant analogies between them in the relationships of the O^- - content, the status of the structural iron content, and hydration of the interlayer.

It is of interest to know whether the apparent interaction between charge-bearing sites at different loci in the kaolinite structure is a direct one, or whether it is mediated by

the interlayer water, or changes in the crystallity of the material. Structural iron and O^--centers are two structural entities which have been proposed to engage in internal redox reactions (Coyne, 1985).

An O^- - center can equivalently be seen to be a trapped hole, one half of a trapped, separated charge pair, or a stored electronic excitation. It seems highly likely that these centers should be associated with oxidizing power. Most iron-bearing clay lattices not only contain structural ferric iron, but also structural ferrous iron, E.S.R. silent. To a significant degree, the distribution of the iron between ferric and ferrous states can be varied over a wide range without significant diminution of the stability of the clay crystal structure. Because of their relatively low activation energy for mobilization, it does not seem improbable that trapped holes could be used to convert structural ferrous to ferric iron under favorable circumstances, thus altering this distribution in a manner dependent on environmental and energetic history. Such a conversion would produce a partial degradation of the energy content of the system and/or a change in the availability of this energy, thus its residence time in the structure. Iron typically is considered to speed relaxation of electronic energy in solids, but it is possible that this relaxation is not complete, but serves instead to produce a meta-stable, semi-relaxed, material.

The interlayer hydration of kaolinites is limited to two molecular layers. That of montmorillonites is considerably more variable. However, the water adsorption isotherm studies of the 1985 MarSAM set (Banin et al., Appendix A) have showed that the isotherm changes shape after two molecular layers of water have been adsorbed, the same number of layers of water as have been associated with ESR changes in kaolinites. The Viking simulation studies of the labeled release, a redox reaction also show a surface activity of the MarSAM's which is highly sensitive to the amount of adsorbed water, particularly at low levels of hydration.

There are three important implications to the MarSAM's study of the results presented in the last two sections. First of all, the studies of the relationship between the environment of structural iron and O^--centers we have accumulated further evidence for the possibility of internal charge exchanges between these entities. Previous evidence for this possibility was derived from the concurrent changes in these entities on heating. The present evidence of such exchanges has been produced at room temperature. Secondly, by means of the TL work with the MarSAM's and the time-dependence of the dehydration-induced luminescence and ESR signal intensities from the kaolinites, further spectroscopic evidence has been accumulated to support the concept of facile interaction between surface and structural electronic properties of clays, both in the ground and the excited states. Such interrelationships between structural and surface electronic properties had previously been seen in kaolinites, in the dependence dehydration-induced luminescence effect on the O^--center content. Lastly, we have produced spectroscopic evidence for inter-relationships between five proven and hypothesized determinants of clay catalytic activity (exchangeable and structural iron, interlayer hydration and thermoluminescence and O^- - population). The meaning of these interrelationships in terms of a model for clay surface reactivity remains to be determined.

Further elucidation of the inter-relationships among the structural entities that have been revealed by our results are of importance also to future Mars Missions, also. They raise a number of significant possibilities relating to determinations of Martian mineralogy and surface geochemistry. 1) Since, using ESR detection, it can be readily shown that the molecular environment of structural iron in clays is readily distinguishable from that in iron oxides and that there are various types of structural iron in clays that are also readily distinguishable from each other, there is good reason to suspect that these

distinctive forms of iron will also show distinctive reflectance signatures. Such signatures will be able to be revealed by NIRA. A well-assigned reflectance signature, discriminating between iron in clays and iron in other oxide/silicate minerals would be helpful both in determining the presence of clays on Mars and the mineralogy of iron on Mars. 2) There is reasonable presumptive evidence to suspect a complex redox relationship that has not been previously investigated, between iron in the structure, iron on the surface of clays, the degree of hydration and their electronic energetic history. This interrelationship needs to be investigated because changes in the redox level should affect the reflectance signature of clays, thus the reflectance signature of planetary surfaces containing clays and 3) because of what the reflectance signature can tell us about the equilibrium, kinetics and energetics of redox reactions on the planetary surface. Knowledge of the redox potential of Mars, for instance, is of importance because of issues of planetary protection.

Use of Correlations Between Electron Spin Resonance and Diffuse Reflectance Spectra to Speciate Surface and Structural Ferric Iron and to Search for O^- - Centers

The discussions in the previous two sections, which relate progress in determining the existence of interactions between a variety of structural entities which are of spectroscopic and surface chemical importance, suggest a means by which these interactions can be sought for and confirmed, using diffuse reflectance coupled with NIRA. That is, the E.S.R. intensities for structural, surface and total ferric iron (the sum of structural and surface) and O^--centers can be used as constituent data for NIRA. In principle, luminescence and thermoluminescence data could be similarly used, but substantial increases would need to be made in our capability for quantitating these properties before the data could be considered reliable. The surface chemical data obtained from the Viking Labled release simulations could be similarly used.

Some initial confirmation of the potential power of this method has already been obtained, also from work done in support of the project on Clay Energetics. E.S.R. and diffuse reflectance spectra of a series of four kaolinites, for which the surface iron component had been altered by selection, physical separation and chemical reduction were measured. The surface ferric iron content was estimated from the amplitude of the broad g = 2 signal and that of the structural ferric from the g = 4 signal. These data were used as constituent data for NIRA. Correlations, for which the confidence ranged from 0.93 - 0.99 were found between the reflectance data and the iron content using both chemical and E.S.R. estimates of total iron and E.S.R. determinations of relative surface and structural ferric iron.

The wavelengths at which the correlations were maximal for the total iron by ESR and by chemical analysis were not the same, as might be expected from the fact that the E.S.R. data is sensitive only to the ferric portion and the chemical analysis data determines the sum of ferric and ferrous iron. Nor were the wavelengths optimally correlated with surface and structural iron the same. Again, as was the case for the NIRA correlating surface iron with reflectance data for the MarSAM's, the sample set examined was very small and these data need confirmation by examination of much larger sample sets and by more redundancy in the constitutent data as provided by different analysis techniques. They do, however, give abundant promise that our present capabilities for being able to determine the reflectance signature of iron in MarSAM's will allow distinctions to be made between total iron, structural ferric and surface ferric.

The results of these examinations of iron in catalytic kaolinites have revealed an additional extremely exciting possiblity. Concentrations of O^- - centers also were determined by E.S.R. Use of these signal amplitudes as a constituent in the auto-search for a correlation, revealed a spectral region of very high overall correlation in the

wavelenth range between 871 and 1038 nm. The correlation was not, by any means, flat over this range, but showed four distinct peaks. The reflectance spectrum, expanded in the wavelength scale for this region of the spectrum is shown in **Figure 14.** These peaks were clearly associated with three small peaks at roughly 2.32, 2.36 and 2.38 μ superposed on an intense continuum of absorption increasing into the red. Bands in this region typically can be associated with combinations of the inner OH stretch with either bending of surface hydroxyls or stretching or bending of SiO bonds (Farmer, 1974 and Hunt and Salisbury, 1970). The small subpeaks could possibly be correlated with sites of isomorphic substitution.

We have consistently held that trapped holes would preferentially situate themselves near the isomorphically substituted centers (Coyne, 1885 and references cited therein). It would not be in the least bit surprising if trapping an electronic excitation at one of these sites were to have a measurable impact on the force constants for a lattice vibrational mode.

It must be reiterated and emphasized once again, that these results have been obtained using a very small sample set. To confirm them will require vigorous testing during the next several years using our prior developed methods of adjusting the O^- - center concentration by use of heat and gamma-irradiation treatments. The relationship between the diffuse reflectance and various luminescence capacities needs also to be developed.

However, even the possibility that these centers might be able to be directly revealed using reflectance data is profoundly significant. Confirmation of such transitions would provide an entirely new category of transitions to be considered in interpreting mineral spectral data. This information would be useful not only in helping to make mineralogical

DIFFUSE REFLECTANCE OF SEVERAL IRON-CONTAINING KAOLINITES IN THE SPECTRAL REGION OF HIGH CORRELATION WITH [O^-] AS DETERMINED BY ESR

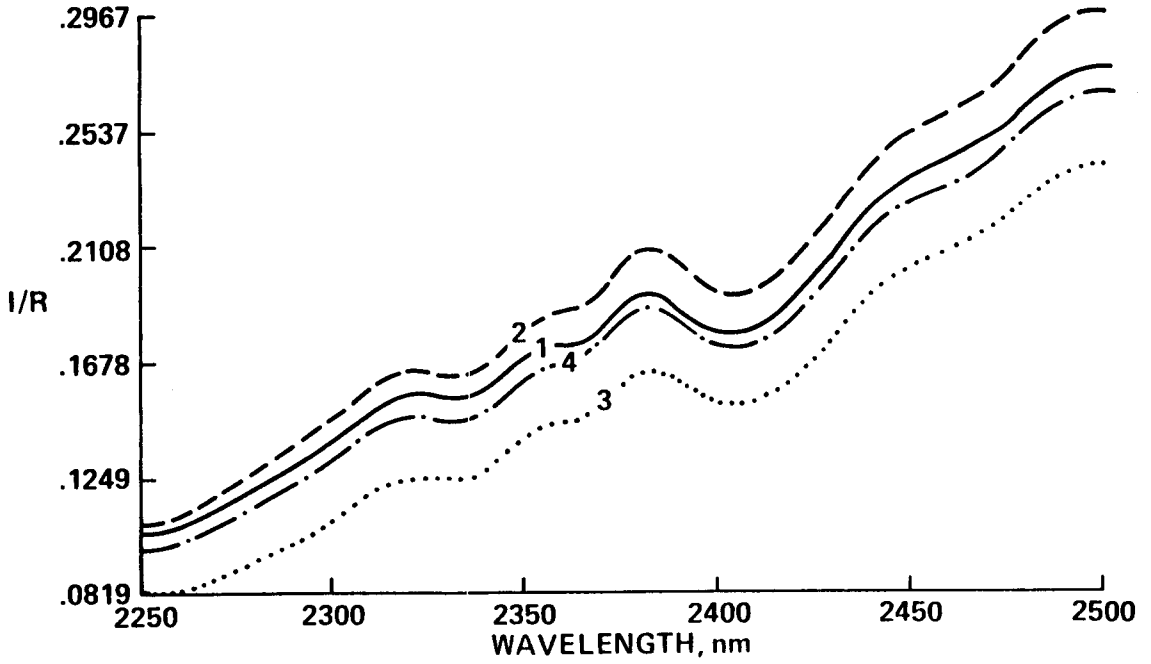

Figure 14

assignments, but also would provide a very powerful tool for assessing remotely the electronic energetic milieu in which these minerals are located. Equally exciting is the potential for discovery of a simply applicable tool for direct visualization of a entity hypothesized to be a mediator for surface chemical reactions.

SUMMARY

In summary of the progress of our NIRA studies of the MarSAMS, we have shown that: 1) the Banin preparation for variably exchanged Fe/Ca clays is spectrally reproducible and stable; 2) the NIRA technique is capable of finding quantifiable relationships between reflectance and total iron; 3) E.S.R. is likely to prove a practical companion technique in conjunction with NIRA for determining reliable analytical wavelengths for both structural and surface ferric iron in clays; 4) O^- - centers may exhibit a measurable reflectance signature and 5) that four variables which are known or thought to be key determiners of clay surface activity appear to show complex structural and spectroscopic inter-relationships.

REFERENCES

Angel, B. R., Cuttler, A. H. and Richards, K. and Vincent, W. E. J. (1977) 'Synthetic kaolinites doped with Fe^{2+} and Fe^{3+} ions' *Clays Clay Minerals* **25,** 381-383.

Angel, B. R. and Hall, P. L. (1973) 'Electron-spin resonance studies of kaolins' *Proc. Int. Clay Conf. Madrid* **47**, 60ff.

Angel, B. R., Jones, J. P. E. and Hall, P. L. (1974) ' Electron spin resonance studies of doped synthetic kaolinites I.' *Clay Minerals* **10**, 247-256.

Angel, B. R., Richards, K. and Jones, R. P. E. (1976) 'The synthesis, morphology and general properties of kaolinites specifically doped with metallic ions and defects generated by irradiation' *Proc. Int. Clay Conf. 1975, Mexico City,* 297-304.

Angel, B. R. and Vincent, W. E. J. (1978) 'Electron spin resonance studies of iron oxides associated with the surface of kaolins' *Clays clay Minerals* **26**, 263-272.

Banin, A. (1973) 'Quantitative ion exchange process for clays'. U.S. Patent no. 3,725,528.

Cariati, F., Erre, L., Micera, G., Piu, P. and Gessa, C. (1983) 'Polarization of water molecules in phyllosilicates in relation to exchange cations as studied by near infrared spectroscopy' *Clays and clay Minerals* **3,** 155-157.

Coyne, L. M. (1985) 'A possible energetic role of mineral surfaces in chemical evolution' *Origins of Life* **15,**161-207.

Coyne, L. M. and Banin, A. (1986) 'Effect of adsorbed iron on thermoluminescence and electron spin resonance spectra of Ca-Fe-exchanged montmorillonite'*Clays and Clay Minerals* **34,** 645-650.

Coyne, L. M., Lahav, N. and Lawless, J. (1981) 'Dehydration-induced luminescence in clay minerals' *Nature* **292,** 819-821.

Farmer, V. C. (1974) Chapter 15 'The layer silicates' in *The Infrared spectra of Minerals* Monograph 4 of the Mineral Society, 41 Queens Gate, London SW7 5 HR.

Goodman, B. A. (1978) 'An investigation by Mossbauer and EPR spectroscopy of the possible presence of iron-rich impurity phases in some montmorillonites'.*Clay Minerals* **13, 351-355.**

Hall, P. L. (1980) 'The application of electron spin resonance spectroscopy to studies of clay minerals: I Isomorphous substitutions and external surface properties' *Clay Minerals* **15,** 321-335.

Hamilton, T. D. S., Munro, i. H. and Walker, G. (1978) 'Luminescence instrumentation' Chapter 3 in *Luminescence Spectroscopy* (M. D, Lumb, editor) 190-192.

Herbillon, A. J., Mestdagh, M. M., Vielvoye, L. and Derouane, E. G. (1976) 'Iron in kaolinite with special reference to kaolinite from tropical soils' *Clay Minerals* **11**, 201-219.

Hunt, G. R. and Salisbury, J. W. (1970) 'Visible and near-infrared spectra of minerals and Rocks: I silicate minerals' *Modern Geology* **1**, 283-300.

Jones, J. P. E. (1974) 'Electron spin resonance studies of doped synthetic kaolinites' PhD. Thesis, Univ. London.

Meads, R. E. and Malden, P. J. (1975) 'Electron spin resonance in natural kaolinites containing Fe^{+3} and other transition metal ions' *Clay Minerals* **10**, 313-345.

Appendix B

APPROACH

NEAR INFRARED REFLECTANCE ANALYSIS

INTRODUCTION

There are two major dilemmas raised by the prior explorations of Mars. water is thought, once, if not still, to have been abundant on Mars, but Viking did not detect abundant adsorbed water in measurements of the volatile content of the soils. Viking determined the existence of abundant iron on Mars, but telescopic studies of surface reflectance do not reveal the signatures characteristic of known crystalline iron oxides. The system of variably Fe/Ca or Fe/H cation-exchanged montmorillonites, called MarSAMs, on which our past and prospective studies are based, has properties which may aid in resolution of both dilemmas.

Whether there are clays on Mars is itself an important issue for several reasons. I) Knowledge that Mars has clays is of interest to planetary geochemists because the presence of clays would be highly suggestive that there was, in fact, abundant water on Mars at some time in the past. 2) Water is tied up in clays, both in the structure itself and as tightly bound

water of hydration of polyvalent exchangeable cations. This water is fully removed only by heating for hours at very high temperatures (References). Such water would only in part have been detected by the Viking experiments, possibly explaining the low volatile content of Martian soils. Finding clays would thus aid in resolving the dilemma of water on Mars, both past and present. 3) Clays are of great interest with respect to the organic geochemistry of any planet, because their properties suit them to catalytic activity toward a wide variety of organic reactions. 4) Clays are of particular interest to the exobiology community, both because of their reaction-promoting capacity in organic synthesis and because of the hypothesis that clays may have served as prototypic inorganic life-forms.

The Banin hypothesis that significant amounts of Martian iron might be associated with the hypothesized Martian smectite clays adds further interest to the possible existence of clays on Mars. There are several possible explanations for the "low profile" of iron in surface reflectance signatures of Mars. One possibility is that Martian iron may occur as very finely divided iron oxides which do not have light absorption properties comparable to those of larger particles of the same material. Another possibility is that the iron oxides are amorphous, or only short-range ordered, rather than crystalline. Our hypothesis is that the iron may exist as the exchangeable cation on a smectite clay and that, further, the presence of the clay may prevent the crystallization of iron in moderate excess of the cation-exchange capacity. A typical montmorillonite, with 100%

exchangeable iron, can account for roughly 33% of the total complement of Martian iron. Significantly more iron may be coated on the surface in forms other than as exchangeable cations, but of insufficient crystallinity to constitute an admixed mineral phase.

This hypothesis specifically associating iron and clay is of particular interest for four reasons. It represents a novel and plausible alternative form for the abundant Martian iron which is consistent with the reflectance signature of the Martian surface (Banin, et al., 1985 and Banin, et al, submitted for publication, Appendix 2). Not only is the exchangeable iron likely to more nearly resemble amorphous, rather than crystalline iron oxides, but also reflectance studies of kaolinites (Jepson,1985) and montmorillonites (Singer, 1982 and Banin, et al., 1985) have shown that iron incorporated into the crystal structure makes a disproportionately small contribution to the reflectance signature in range of d-d transitions. Whereas clays with structural iron content as high as that of nontronite do not simulate Martian reflectance data, (Singer, 1982) less heavily iron-bearing smectites with iron in the crystal lattice, or externally as an exchangeable cation, might conceal a significant portion of the iron-inventory of the Martian surface.

Should iron-adsorbed clays prove to be a significant constituent of the regolith, our model soil has a number of distinctive properties which have strong composition-sensitive implications for the past and present

reactivity of the Martian surface. Past simulations of the Viking labeled release experiments have shown that these materials simulate better the surface chemical activity of Mars than do palagonites, a popular alternative model (Banin and Margules, 1983). Recent updates of these studies indicate a strong dependence of the catalytic activity of the surface toward this reaction on both surface iron and adsorbed water (Banin et al., Appendix 2). This activity is also highly dependent on the Fe/Ca ratio of the exchangeable cations.

In addition to interlayer water, structural and surface iron, another clay structural moeity appears to be a probable contributor, both to the reflectance signature of these materials and to the catalytic activity of the surface. This moeity is electronic energy stored as trapped separated charge pairs, near isomorphously substituted sites in the crystal lattice. These trapped photons will be referred to throughout as O^- - centers. Although all minerals are capable of electronic energy storage, it is likely to be a more significant property of clays than for other minerals because of a) The high energy of electronic excitation for these materials b) The high density of isomorphically substituted sites c) small intrinsic particle size of clays and d) their high specific surface area (Coyne, 1985).

As was discussed in **Section ( )** of the **Appendix I**, recent evidence shows that all four of these entities appear to be inter-related via, as of yet, incompletely defined atomic- or molecular-interactions. Spectroscopic

investigations of both kaolinites and montmorillonites have revealed that altering the population of any one of them has an impact on others. Also, evidence was summarized in **Section ( ) of the Progress** Report which indicates that there may well be features of the reflectance spectra which are attributable to these centers. Comparisons of the surface-iron dependence of the catalytic activity with previously published (Coyne and Banin, 1986) studies of the surface iron dependence of the stored energy content of these materials has revealed some intriguing parallels **(Appendix 2, pp -)**.

SAMPLE SELECTION

For this second stage of our efforts the basic MarSAM set will consist of: 5 Fe/Ca clays ranging from 0 - 100% (0, 20, 50, 80 and 100% Fe) exchangeable iron prepared from SWy - 1, as for the 1985 MarSAM set; 3 Fe/Ca clays, also ranging from 0 - 100 % exchangeable iron (0, 50 and 100% Fe) prepared from Otay or another montmorillonite low in structural iron, a group of clays in which the Fe content exceeds the cation-exchange capacity. Additions of iron will be to levels of 200%, 400% and 600% of the amount needed to saturate the exchange capacity, thus bringing the surface iron content (as Fe_2O_3) to ~5.1%, 10.3%, and 15.4% respectively. Counting the structural iron content, which is about 3.6% as Fe_2O_3 for the SWy, the

highest rate of addition forms a MarSAM which is a full "iron-analog" of the Martian soil. All the above clays will be produced by the Banin method (1973), to ensure reproducibility in treatment and surface composition. In addition, a selection of 6 - 12 assorted montmorillonites for which no chemical treatments will be performed, other than possibly the acid pre-prepurification step will be studied. These latter materials will be included in an ambient temperature NIRA screening to determine the range of wavelengths and intensity ratios over which the spectra of montmorillonites can vary and will be spectroscopically characterized in order to quantitate the various iron species, most particularly those in structural positions.

STUDY OF EFFECTS OF ENVIRONMENTAL CONDITIONS ON SPECTRA

Nira of Adsorbed Water on MarSAMs as a Function of Relative Humidity

An initial set of samples from the MarSAM 1985 suite of clays have been equilibrating for several months at different relative humidities. These are shown in the following table.

TABLE ONE

Eutectic Salt		
Temperature, ^{o}C	**% Humidity**	
Calcium Chloride		20
	4	
($CaCl_2$)		
Potassium Acetate		20
	20	
($KC_2H_3O_2$)		
Calcium Nitrate		24.5
	51	
$Ca(NO_3)\cdot 4H_2O$		

Ammonium Chloride		25
	79.3	
NH_4Cl		
Copper Sulfate		20
	98	
$CuSO_4 \cdot 5H_2O$		

Spectra of these samples will be measured using the Neotec Instrument using the NIR grating in the 1st order to cover the region from 2500 - 1100 and in the second order to cover 1235 - 680 nm and using the 1st order of the visible grating to cover the region from 680 - 380 nm. NIRA will be performed to find a quantitative relationship between reflectance and exchangeable iron and between reflectance and adsorbed water.

Given the results of the analysis of the spectra measured under these conditions, a reassessment will be made of the number of humidities required to give a thorough profiling of the environmental dependence of the spectra of these materials. It is anticipated that four humidities will be measured. The choice of relative humidities will be clustered in the range less than 25%, because of the low water content thought to best represent

Martian conditions, but one high value will be measured in order to determine the upper limit of spectral variation that can be expected from increasing the environmental water content.

Temperature Variation

When the environmental cell is fully operational, the set of materials described above will be re-equilibrated at -20° C in order to establish some expectation of the variablilty of the spectra resulting from temperature changes. On the basis of analysis of this data, two additional temperatures will be selected, at which the humidity studies will be repeated. If deemed important, a decision may be made to try to lower the temperature somewhat further than the -20° lower limit planned.

Atmospheric Variation

The original sample set will be re-examined under a CO_2, or a CO_2/N_2 atmosphere in order to model the effect of these constituents of the Martian atmosphere on the Martian reflectance spectrum. It is also possible that some shifts may be observed in the clay spectra resulting from adsorption of this acidic molecule on the surface ( ). A determination will be made of the necessity of providing a CO_2 atmosphere for all of the measurements, or whether it will be adequate to provide only a CO_2 adsorption correction for the reflectance measurements.

Effects of Radiation

In the **Progress Report, Sections 3a-c,** several prior studies were discussed which gave reason to expect that several structural entities responsible for spectral, and perhaps also surface chemical, activity may be interacting with each other. These entities are structural and surface iron, energy stored as O^- - centers and, perhaps, interlayer water. In order to unravel these interactions it will be necessary to measure the diffuse reflectance and the E.S.R spectra of a group of clays prior to and subsequent to gamma irradiation.

Previous work with kaolinites has shown that a dose of 1 Mrad of radiation from a gamma source is adequate to produce measurable changes in the quantity of energy stored as O^--centers, without producing significant long term radiation damage. The degree of isomorphic substitution of positive charge-deficient Al for Si and Mg or Fe(II) for Al cations in the crystal lattice of a montmorillonite is approximately 100 times that of a typical kaolinite, as estimated from the C.E.C. Whereas, estimated on this basis, the energy storage capacity of the montmorillonites may be higher than those of the kaolinites, it is possible that the high density of storage sites might produce a shorter lifetime for the trapped charges. For these reasons it has been determined that the1 Mrad dose represents as convenient a starting point for investigations as any.

The minimal "core" suite of materials that will be examined is the crude, 100% Ca and 100% Fe forms of the SWy-1 clay and also these same forms prepared from a parent Otay montmorillonite, so as to assess the effect of both surface and structural iron on the energy storage and release capacities. Preferably also the 50% iron forms will be examined, as well as one or two of the Fe/H clays.

To establish a relationship between stored energy and iron, it is necessary that both the reflectance spectra, and the electron-spin resonance signals of the SWy-1 and the Otay montmorillonites, be measured immediately before and after gamma-irradiation and also after intervals, post irradiation, of one week, one month and one year. These measurements will be performed at two temperatures and two relative humidities, as water, too, may be a determining factor in the interactions. Another set of measurements should be performed on materials that have been a) heated to 300^{o} C b) heated to 300^{o} C and then irradiated c) heated to 300^{o} C, irradiated and reheated; in order to determine the reversibility of the reflectance changes to heating and gamma-irradiation. In this way stored energy can be distinguished from radiation damage.

SPECTRAL-CHEMICAL CORRELATIONS

Near infra-red reflectance analysis, NIRA will be performed on the

materials using as constituent data for the regression analysis vs. wavelength the following entities: 1) Total iron by chemical analysis. 2) Total surface iron by chemical analysis. 3) Exchangeable iron. 4) Acid extractable iron. 5) Oxalate extractable iron (Fe_O). 6) Dithionite-Citrate-Bicarbonate (DCB) extractable iron. 7) (Fe_D) (what is this?) 8) surface ferric iron by E.S.R.. 9) structural ferric iron by E.S.R.. 10) O^--centers by E.S.R. New programs purchased for the instrument will allow inter-correlations to be determined for these constituents in order to reveal their hypothesized interdependence.

EXAMINATION OF A SUITE OF VARIED MONTMORILLONITES

For any given parent material, it would be expected, and has been found to be the case (**Figures 8-10 and Tables 3-5**), that at least one, and typically, several optimal analytical wavelengths for correlation with total iron can be found. However, the correlation with total iron was shown to be significantly deteriorated, as might be expected, when a different parent material is included as the basis for a new suite of cation-exchanged materials. The new parent material would have a different amount and speciation of structural iron. In order to determine the sensitivity of the pattern-producing features of the spectrum to structural variability within the class of montmorillonites, we plan to survey a set of crude, or acid-leached montmorillonites and use a variety of components determined

from the elemental analysis as constituents for NIRA in order to find those wavelengths which are characteristic of montmorillonites as a class. For this purpose 6-12 materials will be selected and analyzed chemically, by NIR and by E.S.R.

SUMMARY

The program of research outlined above should advance significantly our understanding of the spectral signal of montmorillonites in general and the variations produced in it by structural and surface ferric and ferrous iron and interlayer water as a function of several environmental conditions that are different between Earth and Mars. In addition we will have collected an extensive data base providing spectral characterization of several structural features (iron, both surface and structural, OH-groups, both structural and from adsorbed water and O^- centers) that are known, or thought to be, influential in directing the surface activity of these important materials. With this data base with which to assess the results of the Viking labeled release simulation studies, it should be possible to gain important insights into the mechanisms of surface reactivity for this important chemical reaction. The results to be gained from these studies will provide a significant body of ground base truth from which to assess: a) the presence of smectite clays on Mars; b) the mineralogical form in which the Martian iron is bound; c) establish upper limits on the present surface water content of Martian soils; d) perhaps provide novel insights on

the Martian surface radiation history; and e) to make strong predictions about the nature of surface chemistry on Mars, if iron-bearing clays are a significant component of the surface mineralogical assemblage.